

used in this study. The mice were maintained on a 12-hour light/12-hour dark cycle and fed *ad libitum*. To induce hypercholesterolemia, wild-type C57BL/6J mice were fed an atherogenic diet, F2HFD1, containing 1.25% cholesterol (Oriental Yeast, Tokyo, Japan) from the beginning one week before administration of any siRNA and throughout the experiment.

To deliver each siRNA, we used InvivoFectamine 2.0 reagent (Invitrogen) according to the manufacturer's instructions. Five mg/kg of each siRNA was formulated with InvivoFectamine 2.0 reagent, and each mouse received one siRNA (siNTC-trl, siApoB-1, siLNA-2, siL2PT-1, siL2PTC-1, siL2PTC-1M, siL2PTC-1L, siL2PT-1M, and siApoB-1C) as an siRNA-InvivoFectamine 2.0 complex via tail vein injection. The physical appearance and body weight of each mouse were recorded during this study. Before an animal was sacrificed, a blood sample was collected from the tail vein using BD Microtainers (BD, Franklin Lakes, NJ). Each of these blood samples was subsequently subjected to centrifugation. TC levels in serum samples were measured using Cholesterol E (Wako, Osaka, Japan) according to the manufacturer's instructions with adjustment for a 96-well microplate. Mice ($N = 3-5$) were sacrificed 2, 7, 14, or 24 days after injection of siRNA. Mice were anesthetized before being sacrificed, and samples of whole blood were collected from each inferior vena cava to measure the activity of AST and ALT and to quantify the BUN and creatinine levels. Next, the liver and kidneys of each animal were harvested to quantify apoB mRNA levels using quantitative PCR; samples of liver tissue and kidney tissue were also collected for histopathological analysis.

Six hours after injection of each siRNA, we collected a blood sample from the tail vein of each mouse. We processed each of these samples to assess serum levels of IFN- α using an IFN- α enzyme-linked immunosorbent assay kit (PBL Interferon Source, Piscataway, NJ) according to the manufacturer's directions.

Harvested liver samples were cut into 2 × 2 mm squares and immediately frozen using liquid nitrogen. For each mouse, one 2 × 2 mm square was put into 1 ml of TRIzol reagent (Invitrogen) for homogenization, and total RNA was isolated in accordance with the manufacturer's protocol accompanying the TRIzol reagent.

Quantitative PCR analysis. We used a High-Capacity cDNA Reverse Transcription Kit (Applied Biosystems, Foster City, CA) to prepare cDNA from 10 μ g of each sample of total RNA extracted from cells or tissues. Each cDNA sample was subjected to Real-Time PCR (StepOnePlus Real-Time PCR System; Applied Biosystems) to measure the relative quantities of APOB, GAPDH, IFIT-1, and OAS-1 expression using SYBR Green reagent (Applied Biosystems) and of SREBP2, α 1 using the TaqMan Gene Expression Assay (Applied Biosystems). The expression levels of target genes were normalized using GAPDH expression as an internal control. The following primer sets were used for quantitative PCR: for mouse ApoB, forward primer 5'-TGGGCAACTT-TACCTATGACTT-3' and reverse primer 5'-AAGGAAATGGCAACGATA-3'; mouse GAPDH, forward primer 5'-CAAAATGGTGAAGTCCGGTGTG-3' and reverse primer 5'-ATTTGATGTTAGTGGG GTCTCG-3'; mouse IFIT-1, forward primer 5'-AGGCTGGAGTGTGCTGAGAT-3' and

reverse primer 5'-TCTGGATTTAACCGGACAG-3'; mouse OAS1, forward primer 5'-CTGACCTGGTGGTGTTCCTT-3' and reverse primer 5'-CCACCATGAACCTCTGGACCT-3'. TaqMan Gene Expression Assay; assay ID for SREBP2, ACAT-1 CYP7 α 1 were Mm01306297_g1, Mm00507463_m1 and Mm00484152_m1, respectively. After an amplification consisting of 40 cycles, relative expression of each target was analyzed with SDS analysis software (Applied Biosystems).

ApoB-100 western blot analysis. Mouse liver tissues were homogenized in Ripa Buffer (Sigma-Aldrich, St Louis, MO) containing complete mini (Roche, Indianapolis, IN). Samples were immediately subjected to centrifugation at 4 °C, 13,000g for 5 minutes. The supernatant of each sample was collected into an Amicon Ultra centrifugal Filters Ultracel-50k (Millipore, Billerica, MA), and the contents of the supernatant were concentrated by centrifugation at 4 °C, 20,000g. The final volume of each retentate was adjusted to 200 μ l with PBS, and the total protein concentration of each sample was determined using a BioRad DC protein assay kit (Lowry method; BioRad, Hercules, CA).

Individual samples (50 μ g) of total protein in liver homogenates were subjected to electrophoresis on a 3–8% NuPAGE Tris-Acetate Gel (Invitrogen) and transferred to a polyvinylidene-fluoride membrane (Millipore). Membranes were then incubated with Blocking One reagent (Nacalai Tesque, Kyoto, Japan) for 12 hours at 4 °C for block nonspecific antibody binding. Membranes were then incubated with primary antibody for mouse apoB-100 or -48 (Meridian Life Science, Inc., Saco, ME) for 2 hours at room temperature. After incubation with primary antibody, each membrane was washed with PBS-containing 0.1% of Tween 20, and then the membranes were incubated with goat anti-rabbit immunoglobulin G secondary antibody conjugated with peroxidase (Santa Cruz Biotechnology, Santa Cruz, CA) dissolved in PBS containing 0.1% of Tween 20-containing 0.5% blocking one reagent for 2 hours at room temperature. Protein bands were visualized using the ECL Advance Western blot detection kit (Amersham Biosciences, Buckinghamshire, UK) according to the manufacturer's directions. Images of each western blot were taken with a LAS-4000 mini image analyzer (FUJIFILM), and the intensity of each band was measured using Image J software (<http://rsbweb.nih.gov/ij/>), which is freely available on the Internet.

Hepatotoxicity and nephrotoxicity assay. To assess the hepatotoxicity associated with each siRNA, we measured the activities of AST and ALT using a GOT-GTP CII kit (Wako) according to the manufacturer's protocol adjusted to 96-well microplate. Results from these assays are presented as AST and ALT activity in IU/L units. As the nephrotoxicities, BUN values in the serum of each sample were measured using a Urea Nitrogen B-test Wako (Wako) kit, and creatinine values in the serum of each sample were measured using FUJI DRI-CHEM CRE-P III with a FUJI DRI-CHEM instrument (FUJIFILM). The Urea Nitrogen B-test Wako was used in accordance with the manufacturer's protocol adjusted to 96-well microplate.

Histopathological analysis. Harvested liver and kidney samples were sectioned and processed for histopathological analysis. Liver and kidney specimens were fixed in 10 %

formalin-PBS (formaldehyde was diluted with PBS, formaldehyde; Wako) for 2 days at room temperature and processed through to paraffin embedding. Routinely, we picked upper and lower lobe regions of the liver and picked kidney tissue including the renal pelvis. All paraffin-embedded tissues were sliced into 5- μ m-thick sections using a microtome (Leica Microsystems, Wetzlar, Germany). These sections were stained with Carrazzi's hematoxylin and eosin (Sakura Finetek USA, Inc., Torrance, CA) solutions for histopathological examination.

Statistical analysis. Therapeutic experiments *in vivo* were performed such that for each time point (day 2, 7, 14, and 24), there were 3–5 mice in each treatment group. A Student's *t*-test was performed for comparison of two arms. Values of $P < 0.05$ or $P < 0.01$ were considered to indicate statistical significance.

Acknowledgments. We thank E. Shibata, M. Inoue, M. Morimoto, and M. Sone who are all affiliated with the National Cerebral and Cardiovascular Center Research Institute, for their technical support. This work was supported by Grants-in-Aid for Scientific Research from the Japanese Ministry of Health, Labor and Welfare (H20-genomu-008 and H23-seisakutansaku-ippan-004) and by the Program for the Promotion of Fundamental Studies in Health Sciences of the National Institute of Biomedical Innovation (NIBIO) of Japan.

Supplementary material

Figure S1. Relative serum total cholesterol (TC) levels on day 40 in the siLNA-2 or siL2PT-1 treated group.

Figure S2. Correlation of apoB mRNA recovery and apoB-100 protein recovery.

Figure S3. Stability of siRNAs toward RNase T.

Figure S4. RIG-I mRNA expression in the liver on day 2 in the siL2PT-1-, siL2PTC-1-, siApoB-1- or siApoB-1C-treated groups.

Figure S5. SREBP2 and ACAT-1 mRNA expression in the liver on day 2 in the siApoB-1- or siApoB-1C-treated groups.

Figure S6. CYP7 α 1 mRNA expression in the liver on day 2.

Materials and Methods.

- Hannon, GJ (2002). RNA interference. *Nature* **418**: 244–251.
- McManus, MT and Sharp, PA (2002). Gene silencing in mammals by small interfering RNAs. *Nat Rev Genet* **3**: 737–747.
- White, PJ (2008). Barriers to successful delivery of short interfering RNA after systemic administration. *Clin Exp Pharmacol Physiol* **35**: 1371–1376.
- Chiu, YL and Pana, TM (2003). siRNA function in RNAi: a chemical modification analysis. *RNA* **9**: 1034–1048.
- De Paula, D, Bentley, MV and Mahato, RI (2007). Hydrophobization and bioconjugation for enhanced siRNA delivery and targeting. *RNA* **13**: 431–456.
- Shim, MS and Kwon, YJ (2010). Efficient and targeted delivery of siRNA *in vivo*. *FEBS J* **277**: 4814–4827.
- Davidson, BL and McCray, PB Jr (2011). Current prospects for RNA interference-based therapies. *Nat Rev Genet* **12**: 329–340.
- Kuwahara, H, Nishina, K, Yoshida, K, Nishina, T, Yamamoto, M, Saito, Y et al. (2011). Efficient *in vivo* delivery of siRNA into brain capillary endothelial cells along with endogenous lipoprotein. *Mol Ther* **19**: 2213–2221.
- Semple, SC, Akinc, A, Chen, J, Sandhu, AP, Mui, BJ, Cho, CK et al. (2010). Rational design of cationic lipids for siRNA delivery. *Nat Biotechnol* **28**: 172–176.
- Love, KT, Mahon, KP, Levins, CG, Whitehead, KA, Querbes, W, Dorkin, JR et al. (2010). Lipid-like materials for low-dose, *in vivo* gene silencing. *Proc Natl Acad Sci USA* **107**: 1864–1869.

- Ge, Q, Dallas, A, Ilves, H, Shorestein, J, Behlke, MA and Johnston, BH (2010). Effects of chemical modification on the potency, serum stability, and immunostimulatory properties of short shRNAs. *RNA* **16**: 118–130.
- Chemolovskaya, EL and Zenkova, MA (2010). Chemical modification of siRNA. *Curr Opin Mol Ther* **12**: 158–167.
- Obika, S, Rahman, SMA, Fujisaka, A, Kawada, Y, Baba, T, and Imanishi, T (2010). Bridged nucleic acids: development, synthesis and properties. *Heterocycles* **81**: 1347–1392.
- Imanishi, T, and Obika, S (2002). BNAs: novel nucleic acid analogs with a bridged sugar moiety. *ChemComm*: 6.
- Eimén, J, Thonberg, H, Ljungberg, K, Frieden, M, Westergaard, M, Xu, Y et al. (2005). Locked nucleic acid (LNA) mediated improvements in siRNA stability and functionality. *Nucleic Acids Res* **33**: 439–447.
- Bramsen, JB, Laursen, MB, Damgaard, CK, Lena, SW, Babu, BR, Wengel, J et al. (2007). Improved silencing properties using small internally segmented interfering RNAs. *Nucleic Acids Res* **35**: 5886–5897.
- Bramsen, JB, Pakula, MM, Hansen, TB, Bus, C, Langkjær, N, Odadzic, D et al. (2010). A screen of chemical modifications identifies position-specific modification by UNA to most potently reduce siRNA off-target effects. *Nucleic Acids Res* **38**: 5761–5773.
- Bramsen, JB, Laursen, MB, Nielsen, AF, Hansen, TB, Bus, C, Langkjær, N et al. (2009). A large-scale chemical modification screen identifies design rules to generate siRNAs with high activity, high stability and low toxicity. *Nucleic Acids Res* **37**: 2867–2881.
- Abdur Rahman, SM, Sato, H, Tsuda, N, Haitani, S, Narukawa, K, Imanishi, T et al. (2010). RNA interference with 2',4'-bridged nucleic acid analogues. *Bioorg Med Chem* **18**: 3474–3480.
- Jurk, M, Chikh, G, Schulte, B, Kritzer, A, Richardt-Pargmann, D, Lampron, C et al. (2011). Immunostimulatory potential of silencing RNAs can be mediated by a non-uridine-rich toll-like receptor 7 motif. *Nucleic Acid Ther* **21**: 201–214.
- Allerson, CR, Sioufi, N, Jarres, R, Prakash, TP, Naik, N, Berdeja, A et al. (2005). Fully 2'-modified oligonucleotide duplexes with improved *in vitro* potency and stability compared to unmodified small interfering RNA. *J Med Chem* **48**: 901–904.
- Samuel-Abraham, S and Leonard, JN (2010). Staying on message: design principles for controlling nonspecific responses to siRNA. *FEBS J* **277**: 4828–4836.
- Goldstein, JL (2001). Laskers for 2001: knockout mice and test-tube babies. *Nat Med* **7**: 1079–1080.
- Durrington, P (2003). Dyslipidaemia. *Lancet* **362**: 717–731.
- Soutschek, J, Akinc, A, Bramlage, B, Charisse, K, Constien, R, Donoghue, M et al. (2004). Therapeutic silencing of an endogenous gene by systemic administration of modified siRNAs. *Nature* **432**: 173–178.
- Khvorov, A, Reynolds, A and Jayasena, SD (2003). Functional siRNAs and miRNAs exhibit strand bias. *Cell* **115**: 209–216.
- Schwarz, DS, Hutvagner, G, Du, T, Xu, Z, Aronin, N and Zamore, PD (2003). Asymmetry in the assembly of the RNAi enzyme complex. *Cell* **115**: 199–208.
- Kennedy, S, Wang, D and Ruvkun, G (2004). A conserved siRNA-degrading RNase negatively regulates RNA interference in *C. elegans*. *Nature* **427**: 645–649.
- Volkov, AA, Kruglova, NS, Meschaninova, MI, Veryninova, AG, Zenkova, MA, Vlassov, VV et al. (2009). Selective protection of nuclease-sensitive sites in siRNA prolongs silencing effect. *Oligonucleotides* **19**: 191–202.
- Mook, OR, Baas, F, de Wissel, MB and Fluiter, K (2007). Evaluation of locked nucleic acid-modified small interfering RNA *in vitro* and *in vivo*. *Mol Cancer Ther* **6**: 833–843.
- Liu, L, Botos, I, Wang, Y, Leonard, JN, Shiloach, J, Segal, DM et al. (2008). Structural basis of toll-like receptor 3 signaling with double-stranded RNA. *Science* **320**: 379–381.
- Judge, AD, Bola, G, Lee, AC and MacLachlan, I (2006). Design of noninflammatory synthetic siRNA mediating potent gene silencing *in vivo*. *Mol Ther* **13**: 494–505.
- Homung, V, Guenther-Biller, M, Bourquin, C, Ablasser, A, Schlee, M, Uematsu, S et al. (2005). Sequence-specific potent induction of IFN- α by short interfering RNA in plasmacytoid dendritic cells through TLR7. *Nat Med* **11**: 263–270.
- McCarroll, J, Baigude, H, Yang, CS and Rana, TM (2010). Nanotubes functionalized with lipids and natural amino acid dendrimers: a new strategy to create nanomaterials for delivering systemic RNAi. *Bioconjug Chem* **21**: 56–63.
- Aronin, N (2006). Target selectivity in mRNA silencing. *Gene Ther* **13**: 509–516.
- Jackson, AL, Burchard, J, Leake, D, Reynolds, A, Schelter, J, Guo, J et al. (2006). Position-specific chemical modification of siRNAs reduces "off-target" transcript silencing. *RNA* **12**: 1197–1205.
- Carthew, RW and Sontheimer, EJ (2009). Origins and Mechanisms of miRNAs and siRNAs. *Cell* **136**: 642–655.
- Matranga, C, Tomari, Y, Shin, C, Bartel, DP and Zamore, PD (2005). Passenger-strand cleavage facilitates assembly of siRNA into Ago2-containing RNAi enzyme complexes. *Cell* **123**: 607–620.
- Leuschner, PJ, Ameres, SL, Kueng, S and Martinez, J (2006). Cleavage of the siRNA passenger strand during RISC assembly in human cells. *EMBO Rep* **7**: 314–320.
- Rossi, JJ (2009). Cholesterol paves the way for topically applied viricides. *Cell Host Microbe* **5**: 6–7.
- Ambardekar, VV, Han, HY, Varney, ML, Vinogradov, SV, Singh, RK and Vetro, JA (2011). The modification of siRNA with 3' cholesterol to increase nuclease protection and suppression of native mRNA by select siRNA polyplexes. *Biomaterials* **32**: 1404–1411.

42. Haley, B and Zamore, PD (2004). Kinetic analysis of the RNAi enzyme complex. *Nat Struct Mol Biol* 11: 599–606.
43. Marques, JT, Devosse, T, Wang, D, Zamanian-Daryoush, M, Serbinowski, P, Hartmann, R et al. (2006). A structural basis for discriminating between self and nonself double-stranded RNAs in mammalian cells. *Nat Biotechnol* 24: 559–565.
44. Kato, H, Takeuchi, O, Mikamo-Sato, E, Hirai, R, Kawai, T, Matsushita, K et al. (2008). Length-dependent recognition of double-stranded ribonucleic acids by retinoic acid-inducible gene-1 and melanoma differentiation-associated gene 5. *J Exp Med* 205: 1601–1610.
45. Gao, S, Dagnaes-Hansen, F, Nielsen, EJ, Wengel, J, Besenbacher, F, Howard, KA et al. (2009). The effect of chemical modification and nanoparticle formulation on stability and biodistribution of siRNA in mice. *Mol Ther* 17: 1225–1233.
46. Caffrey, DR, Zhao, J, Song, Z, Schaffer, ME, Haney, SA, Subramanian, RR et al. (2011). siRNA off-target effects can be reduced at concentrations that match their individual potency. *PLoS ONE* 6: e21503.



Molecular Therapy–Nucleic Acids is an open-access journal published by *Nature Publishing Group*. This work is licensed under the Creative Commons Attribution-Noncommercial-No Derivative Works 3.0 Unported License. To view a copy of this license, visit <http://creativecommons.org/licenses/by-nc-nd/3.0/>

Supplementary Information accompanies this paper on the Molecular Therapy–Nucleic Acids website (<http://www.nature.com/mtna>)



Hybridizing ability and nuclease resistance profile of backbone modified cationic phosphorothioate oligonucleotides

S.M. Abdur Rahman^{a,*}, Takeshi Baba^b, Tetsuya Kodama^b, Md. Ariful Islam^a, Satoshi Obika^{b,*}

^a Department of Clinical Pharmacy and Pharmacology, Faculty of Pharmacy, University of Dhaka, Dhaka 1000, Bangladesh

^b Graduate School of Pharmaceutical Sciences, Osaka University, 1-6 Yamadaoka, Suita, Osaka 565-0871, Japan

ARTICLE INFO

Article history:

Received 21 March 2012

Revised 1 May 2012

Accepted 2 May 2012

Available online 12 May 2012

Keywords:

Phosphorothioate

Backbone modification

Aminoalkyl moiety

UV melting experiment

Nuclease resistance

ABSTRACT

Various stereochemically pure cationic phosphorothioate oligonucleotides bearing aminoalkyl moieties were synthesized, and their duplex-forming ability against single-stranded DNA (ssDNA), single-stranded RNA (ssRNA) and triplex-forming ability against double-stranded DNA (dsDNA) were evaluated by UV melting experiments. The cationic Rp stereoisomers showed improved duplex-forming ability against ssDNA, triplex-forming ability against dsDNA and nuclease stability.

© 2012 Elsevier Ltd. All rights reserved.

1. Introduction

Chemically modified oligonucleotides are increasingly used in antisense,¹ antigene,² RNA interference (RNAi)³ and other genomic technologies such as nucleic acid nanotechnology and drug target validation.^{4,5} One of the simplest chemical modifications of oligonucleotides is the phosphorothioate (PS) modification in which a non-bridging oxygen on phosphorus is replaced by a sulfur atom.⁶ PS oligodeoxynucleotides (ODN) showed great promises in antisense technology because of their ease of synthesis and high resistance to nuclease degradation.⁷ The first antisense drug, Vitravene™ (Formivirsen), containing PS-ODN was approved by the FDA in 1998 for the treatment of cytomegalovirus retinitis,⁸ and several others are in clinical trials.⁹ Derivatives of PS-ODNs have recently been applied in sequence specific DNA cleavage¹⁰ and construction of DNA nanostructures.¹¹ However, one of the major problems encountered in the use of PS-ODNs is their low hybridizing ability against complementary strands. Duplex-forming ability against ssDNA or ssRNA is reduced gradually^{12,13} and triplex-forming ability is greatly diminished or totally lost upon PS modification.^{14,15} To overcome these problems, modifications such as introduction of cationic residues, polyamines and stacking enforcers on the nucleobase have been accomplished.^{16–21} These strategies improved the duplex-forming ability in many cases;

however, triplex-forming ability was either reduced or not determined. Alternatively, mixing of natural and synthetic polyamines of various sizes has also been investigated for improving hybrid stability.^{22,23}

Introduction of an additional functional moiety on the backbone to improve the hybridizing ability of ODNs and their nuclease resistance was also investigated.²⁴ Grafting of cationic functional moieties on the backbone of natural β -ODNs was found to destabilize duplexes/triplexes, whereas grafting with the non-natural α -ODNs was shown to improve the duplex- and triplex-forming abilities.²⁵ The stabilization of hybrids by cationic moieties lies in their ability to neutralize the repulsive negative charges on the phosphate backbones and generate an electrostatic interaction with the anionic phosphate backbone. Cationic moieties conjugated to ODNs are also known to improve the uptake of ODNs into cells.²⁶ Among the various modifications engineered on the backbone, most have been performed on the usual phosphodiester linkage and only very few attempts were undertaken to functionalize the sulfur atom of PS-ODN.^{10,11,27,28} Labeling of the sulfur atom of PS-ODN was achieved by some groups using alkylating agents containing haloacetamides, aziridine sulfonamides, γ -bromo- α,β -unsaturated carbonyl compounds²⁷ or maleimidyl derivatives.²⁸ However, incorporation of such groups on the sulfur atom resulted in destabilization of the duplex and no data related to triplex formation has been reported.

The high nuclease resistance of PS-ODN and the lack of sufficient examples of backbone modification prompted us to investigate the conjugation of cationic amino groups on the backbone of PS-ODN. Therefore, we planned to introduce several cationic amino

* Corresponding authors. Tel.: +880 2 9661900 70x8166 (S.M.A.R.); tel.: +81 6 6879 8200; fax: +81 6 6879 8204 (S.O.).

E-mail addresses: rahman_du@yahoo.com (S.M.A. Rahman), obika@phs.osaka-u.ac.jp (S. Obika).

linkers of different chain lengths to the PS-ODN based on a post-synthetic modification protocol (Scheme 1).²⁸ Herein, we describe the introduction of various monoamines and diamines of variable lengths onto the PS backbone and their effects on hybridization and nuclease resistance profiles.

2. Results and discussion

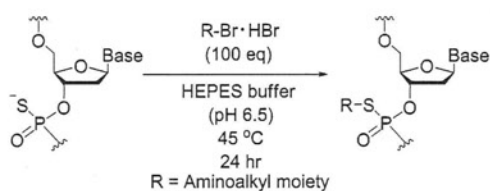
2.1. Conjugation of aminoethyl moiety to oligonucleotide containing purine bases

Initially, a 12 mer PS-ODN, 5'-d(GCGTTTsTTTGCT)-3' (**S1**) containing one phosphorothioate modification at the middle (labeled as s), was used for introducing the 2-aminoethyl group on the sulfur atom according to the reported procedure.²⁸ The corresponding aminoethyl PS-ODN, 5'-d(GCGTTTs-R TTTGCT)-3', R = -CH₂CH₂NH₂ (**S2**) was obtained, together with a number of cleavage products resulting from alkylation of the guanine residues.²⁹ The purified diastereoisomeric mixtures of aminoethyl PS-ODN were hybridized with 12 mer complementary ssDNA and ssRNA and the thermal stability or UV melting temperature (T_m) was determined. The thermal stability of the duplex formed with aminoethyl PS-ODN against ssDNA is equal, and that against ssRNA was slightly lower, compared to the T_m s obtained for non-alkylated PS-ODN. The unmodified natural phosphodiester ODN, 5'-d(GCGTTTTT TGCT)-3' (**S3**) possessed higher T_m than the PS-ODN and aminoethyl PS-ODN.³⁰

2.2. Conjugation of aminoalkyl moieties to the polypyrimidine oligonucleotide

Because of the partial formation of cleavage products due to guanine-alkylation and subsequent purification problems, we decided to use a sequence without guanine residue and ultimately selected two separate stereochemically pure Sp and Rp PS-ODNs 5'-d(CCCTTTsTTTCCT)-3' (**1Sp**, **1Rp**) bearing a polypyrimidine tract.³¹ Stereochemistry of the PS-ODNs **1** were determined by comparing the nuclease stability against snake venom phosphodiesterase which cleaves Rp isomer faster than Sp isomer.³² A number of monoamines and diamines with variable alkyl chains were conjugated with the stereochemically pure PS-ODNs using the reported protocol²⁸ and the corresponding aminoalkyl PS derivatives **2Sp–10Sp** and **2Rp–10Rp** were obtained in 24–55% yields (Table 1). The aminoalkyl PS-ODNs were purified by RP-HPLC and characterized by MALDI-TOF mass spectrometry (for purification, yield and MALDI-TOF mass data see the Supplementary data).

The synthesized cationic PS-ODNs **2Sp–10Sp** and **2Rp–10Rp** were then investigated for their duplex-forming ability against complementary ssDNA and ssRNA targets and the results are compared to the parent PS-ODNs **1Sp** and **1Rp**, respectively (Tables 2 and 3). The T_m of ODNs **1Sp** and **1Rp** against ssDNA under specified conditions (Table 2) was found to be identical (42 °C). Alkylation by the 2-aminoethyl moiety to the Sp- isomer **1Sp** (ODN **2Sp**) decreased the T_m slightly, while that of the Rp-isomer (**2Rp**) increased the T_m by 3 °C. Increasing the aminoalkyl chain length of the Sp-



Scheme 1. Conjugation of aminoalkyl groups to phosphorothioate triester.

Table 1
Yields of aminoalkylated phosphorothioate oligonucleotides

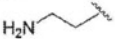
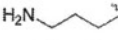





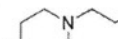

Oligonucleotide	Yield (%)	
	Sp	Rp
5'-d(CCCTTT _{s,r} TTTCCC)-3'		
R= (2)	39	49
(3)	41	34
(4)	49	42
(5)	53	43
(6)	44	49
(7)	24	39
(8)	28	41
(9)	55	55
(10)	33	53

isomers, that is introduction of 3-aminopropyl, 4-aminobutyl, 5-aminopentyl and 6-aminoethyl groups (**3Sp–6Sp**) destabilized the duplex to a larger extent than that observed for the short 2-aminoethyl chain (**2Sp**).

Cationization of **1Sp** by acyclic and cyclic diamino moieties (**7Sp–10Sp**) also destabilized the duplex and the corresponding Rp-ODNs (**7Rp–10Rp**) exhibited enhanced duplex stability (T_m increased by 3 °C). For most of the Rp conjugates, thermal stability was equal to or slightly improved than that of the natural phosphodiester ODN **11**. Melting temperatures in the absence of salt (NaCl) were also recorded for **2Sp**, **2Rp** and **9Sp**, **9Rp** and the results were compared to those obtained for **1Sp** and **1Rp**. The ΔT_m of both **2Rp** and **9Rp** compared to **1Rp** was found to be +3 °C and that for the Sp-isomers **2Sp** and **9Sp** was -2 °C compared to **1Sp** (data not shown). Therefore, the increase and the decrease of T_m in the absence or presence of NaCl were similar, indicating that these changes of T_m s are related to the structure of the ODNs. The increase of T_m against ssDNA using Rp-ODNs might be very interesting for constructing recently reported protein based nanostructures¹¹ or for designing amino modified ODN probes for DNA microarrays.³³ The difference of T_m between Sp- and Rp-isomers is significant; for example for **7Rp** and **7Sp** the difference is 5 °C by a single modification. Anionic sulfur atoms of Sp- and Rp-ODNs are faced to the inside and the outside of the duplex, respectively. Inward orientation is expected to cause a negative charge repulsion between anionic sulfur atom and negative charge present in complementary strand.³⁴ Aminoalkylation neutralizes negative charge at the sulfur atom and decreases the unfavorable repulsion. This neutralization effect stabilized duplexes formed with the Rp-ODNs whereas the stabilization effect might be weak in case of outward-oriented Sp-ODNs.

Against the complementary ssRNA (Table 3), all aminoalkyl functional Sp PS-ODNs (**2Sp–10Sp**) showed decreased T_m compared to the parent ODN **1Sp**. Rp-isomers (**2Rp–10Rp**) also afforded slightly decreased or equal T_m . These results show that irrespective of the stereoisomers, modification of a sulfur atom on a phosphorothioate linkage by an aminoalkyl moiety usually is detrimental for A-form DNA/RNA duplex stability and destabilization is more pronounced in duplexes formed by Sp-conformers. This destabilization effect may result from an unfavorable steric interaction or disturbance of the hydration pattern found in A-form duplexes.³⁵

Table 2
Thermal stability of duplexes formed by cationic Sp and Rp isomers with complementary ssDNA^{a,b}




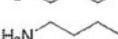



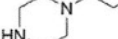
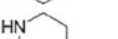
Oligonucleotide		Sp		Rp		
		T_m^c	ΔT_m	T_m^c	ΔT_m	
5'-d(CCCTTT _s TTTCCC)-3'	(1)	42	–	42	–	
5'-d(CCCTTT _{s-r} TTTCCC)-3'						
R=		(2)	41	–1	45	+3
		(3)	40	–2	43	+1
		(4)	40	–2	44	+2
		(5)	39	–3	44	+2
		(6)	37	–5	42	0
		(7)	40	–2	45	+3
		(8)	40	–2	45	+3
		(9)	40	–2	45	+3
		(10)	41	–1	45	+3

^a Target ssDNA: 5'-d(AGGAAAAAAGGG)-3'.

^b T_m values of the natural oligonucleotide 5'-d(CCCTTTTTCCT)-3' (**11**) for ssDNA is 44 °C.

^c T_m condition: 10 mM sodium phosphate buffer (pH 7.2), 100 mM NaCl, 4 μ M each oligonucleotide.

Table 3
Thermal stability of duplexes formed by cationic Sp and Rp isomers with complementary ssRNA^{a,b}

Oligonucleotide		Sp		Rp		
		T_m^c	ΔT_m	T_m^c	ΔT_m	
5'-d(CCCTTT _s TTTCCC)-3'	(1)	46	–	46	–	
5'-d(CCCTTT _{s-r} TTTCCC)-3'						
R=		(2)	43	–3	45	–1
		(3)	43	–3	46	0
		(4)	43	–3	45	–1
		(5)	42	–4	44	–2
		(6)	41	–5	43	–3
		(7)	44	–2	45	–1
		(8)	44	–2	46	0
		(9)	44	–2	46	0
		(10)	43	–3	45	–1

^a Target ssRNA: 5'-r(AGGAAAAAAGGG)-3'.

^b T_m values of the natural oligonucleotide 5'-d(CCCTTTTTCCT)-3' (**11**) for ssRNA is 48 °C.

^c T_m condition: 10 mM sodium phosphate buffer (pH 7.2), 100 mM NaCl, 4 μ M each oligonucleotide.

It is possible that the cationic Rp-isomers enhanced the stability of B-form DNA/DNA duplexes while destabilizing the A-form DNA/RNA duplex due to the fact that in the case of the A-form duplex, long lived hydration patterns are present in the deep major groove and involve a sequence independent water bridge between the proRp oxygen atom and the adjacent phosphate group,³⁶ whereas such interactions are absent in B-form duplexes because the corresponding distance is too long.³⁷

Next, we investigated the triplex formation at pH 5.5 towards 22-bp dsDNA target bearing a homopurine-homopyrimidine tract. The same ODNs used in duplex studies were employed for the

triplex study and the results are summarized in Table 4. All the aminoalkyl conjugates of the Sp-isomer caused destabilization of the triplex as shown by the ΔT_m values. In remarkable contrast, all aminoalkyl Rp-conformers increased the T_m values with respect to that obtained for **1Rp**. The increase of T_m varies depending on the size and structural features of the aminoalkyl substituents and the highest increase of T_m ($\Delta T_m = +6$ °C) was noted for ODN **8Rp** consisting of a 2-(3-aminopropyl)aminoethyl moiety. Another notable increase of T_m was found for the diamine derivative **7Rp** ($\Delta T_m = +5$ °C) bearing the 2-(2-aminoethyl)aminoethyl moiety. The increase of T_m s using **7Rp** and **8Rp** is also greater than that

Table 4
Thermal stability of triplexes formed by cationic Sp and Rp isomers with complementary dsDNA^{a,b}

Oligonucleotide	Sp		Rp		
	T_m^c	ΔT_m	T_m^c	ΔT_m	
5'-d(CCCTTT _s TTTCCC)-3' 5'-d(CCCTTT _{s,r} TTTCCC)-3'	(1)	26	–	25	–
R=					
	(2)	24	–2	29	+4
	(3)	24	–2	29	+4
	(4)	24	–2	27	+2
	(5)	24	–2	27	+2
	(6)	23	–3	27	+2
	(7)	25	–1	30	+5
	(8)	25	–1	31	+6
	(9)	24	–2	28	+3
	(10)	23	–3	27	+2

^a Target dsDNA: 5'-d(GCAGCGGGAAAAAGGAGCAGC)-3'/3'-d(CGTCCGCTTTTCTCTCGTCG)-5'.

^b T_m values of the natural oligonucleotide 5'-d(CCCTTTTCTCT)-3' (**11**) for dsDNA is 29 °C.

^c T_m condition: 7 mM sodium phosphate buffer (pH 5.5), 140 mM KCl, 10 mM MgCl₂, 1.5 μM Oligonucleotide.

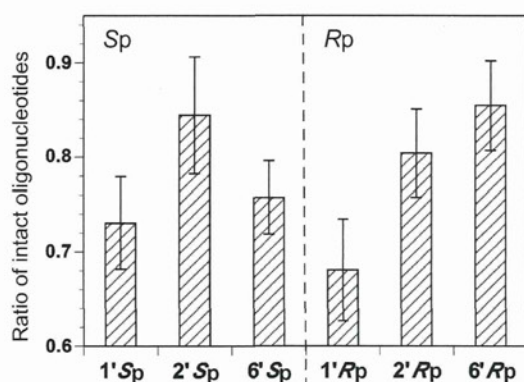


Figure 1. Enzymatic stability of 5'-d(CCCTTTsT)-3' (**1'Sp**, **1'Rp**) and 5'-d(CCCTTTs-rT)-3' (**2'Sp**, **2'Rp** and **6'Sp**, **6'Rp**) against *Crotalus Admanteus* Venom Phosphodiesterase (CAVP). Experiments were carried out at 37 °C for 15 min in buffer containing 50 mM Tris-HCl (pH 7.5), 10 mM MgCl₂, each ODNs and CAVP.

observed for natural unmodified phosphodiester ODN **11**. The T_m observed for **8Rp** was 2 °C higher than that obtained for the natural phosphodiester ODN **11**. This increase of T_m by the Rp congeners might arise from neutralization of the repulsive forces in the phosphate backbone via cationization of the third strand or via favorable intra or interstrand interaction between positively charged amino groups and phosphate oxygens, similar to that obtained using polyamines.³⁸

Triplex formation using phosphorothioate ODN is inefficient in most cases and usually a large decrease of T_m is observed upon PS modification, which restricts the use of PS-ODN in antigene technology.^{14,15} However, the incremental increase of T_m by 4 or 5 °C by single 3-(2-aminoethyl)aminoethyl or 2-(2-aminopropyl)aminoethyl linked PS-ODN implies that cationic PS-ODNs might be interesting candidates for antigene technology. This property along with the increased T_m over natural unmodified ODN might be very interesting for designing triplex-forming oligonucleotides (TFO) for antigene technologies and recently reported site specific DNA cleavage using PS-TFO.¹⁰

2.3. Evaluation of nuclease stability of the conjugated oligonucleotides

Conjugation of a functional moiety to the sulfur atom of PS-ODN is effective in improving the nuclease resistance property.¹⁰ We evaluated the nuclease stability of aminoalkylated PS-ODN using 3'-exo nuclease [*Crotalus Admanteus* Venom Phosphodiesterase (CAVP)]. First, we attempted to investigate the stability of ODN **8Rp**, which showed the highest triplex-forming ability, and its diastereomer **8Sp**. However, unexpectedly, **8Rp** and **8Sp** were heat-labile. Therefore, **8Sp**, **8Rp** were substituted for **2Sp**, **2Rp** and **6Sp**, **6Rp** bearing amino moieties at the same position as **8Sp**, **8Rp**. For easier comparison of the nuclease stability of aminoalkylated PS-ODNs, 12 mer ODNs were digested from the 3'-position in advance to give 7 mer ODNs, 5'-d(CCCTTTsT)-3' (**1'Sp**, **1'Rp**), 5'-d(CCCTTTs-rT)-3' (R = -(CH₂)₂NH₂, **2'Sp**, **2'Rp**), (R = -(CH₂)₆NH₂, **6'Sp**, **6'Rp**). The resulting ODNs were incubated with CAVP once again and the ratio of the remaining ODNs at 15 min was evaluated (Fig. 1). The Sp PS-ODN **1'Sp** showed slightly higher stability than Rp PS-ODN **1'Rp**. The aminoalkylated Sp PS-ODNs (**2'Sp**, **6'Sp**) showed comparable or higher nuclease stability than **1'Sp**. In contrast, aminoalkylated Rp PS-ODN (**2'Rp**, **6'Rp**) showed further enhanced nuclease stability compared to **1'Rp**. Interestingly, the stability of the Rp and Sp isomers was reversed by conjugation of an aminohexyl moiety. Aminoalkylation on the sulfur atom is effective to improve the nuclease stability of PS-ODN, notably Rp-isomers.

3. Conclusion

In conclusion, we have successfully introduced various aminoalkyl moieties to the sulfur group of stereodefined PS-ODNs. The aminoalkyl conjugated Rp-isomers of phosphorothioate exhibited increased stabilization of DNA duplexes while the Sp-conformers destabilized the duplexes. Both the cationic Rp- and Sp-isomers showed decreased affinity towards RNA. Triplex formation was enhanced by all the aminoalkyl functionalized Rp-isomers. The most significant triplex stabilization was observed with 2-(3-aminopropyl)aminoethyl and 2-(2-aminoethyl)aminoethyl linked Rp-PS-ODNs. We also revealed that the alkylation of PS-ODNs is effective to enhance the nuclease stability and increase of nuclease stability

is more pronounced for Rp isomers. Considering all the results we assume that cationic Rp-PS-ODNs might be an interesting candidate for DNA based technologies such as DNA microarray, DNA nanostructures and antigene technologies.

4. Experimental section

4.1. General information

Melting points are uncorrected. ^1H NMR (400 MHz) and ^{13}C NMR (100 MHz) were recorded on a JEOL JNM-ECS-400 spectrometer. Chemical shifts are reported in parts per million downfield from residual solvent of D_2O (4.79 ppm) for ^1H NMR or methanol- d_4 (49.0 ppm) for ^{13}C NMR. Mass spectra were measured on JEOL JMS-700 mass spectrometers. MALDI-TOF mass spectra were recorded on a Bruker Daltonics Autoflex II TOF/TOF mass spectrometer. For high performance liquid chromatography (HPLC), Shimadzu LC-10AT_{VP}, SPD-10A_{VP} and CTO-10_{VP} were used. Thermal denaturation experiments were carried out on Shimadzu UV-1650 and UV-1800 spectrophotometers equipped with a T_m analysis accessory. Oligonucleotide **1** was purchased from GeneDesign Inc. Aminoalkylating reagents were purchased (ethyl and propyl) or synthesized (others except for 6-bromohexylammonium bromide)^{39–41} as the respective ammonium bromides.

4.2. Synthesis of 6-bromohexylammonium bromide

6-Aminoethanol (500 mg, 4.27 mmol) was slowly added to a stirring 48% hydrogen bromide solution (5.1 mL) at 0 °C and the resulting mixture was stirred at 80 °C for 20 h. The mixture was concentrated and crystallized from toluene/ethanol = 50/1 to give 6-bromohexylammonium bromide (674 mg, 2.6 mmol, 61%) as a white solid.

Mp 130–133 °C (toluene/ethanol = 50/1). ^1H NMR (400 MHz, D_2O): δ 1.37–1.48 (4H, m), 1.61–1.68 (2H, m), 1.82–1.87 (2H, m), 2.96 (2H, t, $J = 8$ Hz), 3.48 (2H, t, $J = 7$ Hz). ^{13}C NMR (100 MHz, CD_3OD): δ 26.6, 28.4, 28.6, 33.6, 34.2, 40.6. MS (FAB) m/z 180 ($\text{M}-\text{Br}^-$). HRMS (FAB): Calcd for $\text{C}_6\text{H}_{15}\text{NBr}$ ($\text{M}-\text{Br}^-$): 180.0382. Found: 180.0395.

4.3. Synthesis of aminoalkylated PS-ODNs

Each aminoalkylation reagent (1.0 M, 2 μL , 2 μmol) in DMF (for ODN **2–6**) or H_2O (for ODN **7–10**) was added to a solution of ODN **1** (10 nmol) in 22 mM HEPES buffer (18 μL , pH 6.5) and the reaction mixture was incubated at 45 °C for 24 h. After completing the reaction, ODN was precipitated by adding ethanol (100 μL). The mixture was kept at 0 °C for 15 min, centrifuged at 13,200 rpm for 15 min at 4 °C, and the resulting supernatant solution was removed. The obtained ODN was purified by RP-HPLC and characterized by MALDI-TOF mass spectrometry.

4.4. Preparation of enzymatically digested ODNs

Crotalus Admanteus Venom Phosphodiesterase (CAVP, Pharmacia Biotech) (1.3 μg for **1'** and **6'Rp**, 4.5 μg for **2'Sp**, 4.1 μg for **2'Rp**, 1.3 μg for **6'Sp**) was added to a solution of 3.3 μM ODN (5.0 nmol for **1'** and **6'R**, 4.5 nmol for **2'Sp**, 4.1 nmol for **2'Rp**, 5.1 nmol for **6'Sp**) in 25 mM Tris–HCl buffer (pH 8.5 for **1'**, **6'**, pH 7.5 for **2'**) containing 4.0 mM MgCl_2 . The reaction mixture was incubated at 37 °C for 30 min and heated to 90 °C for 30 min to inactivate the nuclease. The mixture was concentrated and purified by RP-HPLC.

4.5. Evaluation of nuclease stability

Crotalus Admanteus Venom Phosphodiesterase (CAVP, Pharmacia Biotech) (0.40 μg) was added to a solution of 3.3 μM ODN

(0.40 nmol) in 50 mM Tris–HCl buffer (pH 7.5) containing 10 mM MgCl_2 . The reaction mixture was incubated at 37 °C for 15 min and heated to 90 °C for 5 min to inactivate the nuclease. The amount of intact ODN was quantified by HPLC.

Acknowledgments

A part of this work was supported by the bilateral joint projects conducted by Japan Society of Promotion of Science (JSPS) and University Grants Commission of Bangladesh (UGC)

Supplementary data

Supplementary data associated with this article can be found, in the online version, at <http://dx.doi.org/10.1016/j.bmc.2012.05.009>.

References and notes

- Crooke, S. T. *Annu. Rev. Med.* **2004**, *55*, 61.
- Buchini, S.; Leumann, C. J. *Curr. Opin. Chem. Biol.* **2003**, *7*, 717.
- Novina, C. D.; Sharp, P. A. *Nature* **2004**, *430*, 161.
- Yan, H. *Science* **2004**, *306*, 2048.
- Taylor, M. F.; Wiederholt, K.; Sverdrup, F. *Drug Discovery Today* **1999**, *4*, 562.
- Stein, C. A.; Cheng, Y.-C. *Science* **1993**, *261*, 1004.
- Eckstein, F. *Annu. Rev. Biochem.* **1985**, *54*, 367.
- Marwick, C. J. *Am. Med. Assoc.* **1998**, *280*, 871.
- Yamamoto, T.; Nakatani, M.; Narukawa, K.; Obika, S. *Future Med. Chem.* **2011**, *3*, 339.
- Vekhoff, P.; Halby, L.; Oussedik, K.; Dallavalle, S.; Merlini, L.; Mahieu, C.; Lansiaux, A.; Bailly, C.; Boutorine, A.; Pisano, C.; Giannini, G.; Alloati, D.; Arimondo, P. B. *Bioconjugate Chem.* **2009**, *20*, 666.
- Lee, J. H.; Wong, N. Y.; Tan, L. H.; Wang, Z.; Lu, Y. J. *Am. Chem. Soc.* **2010**, *132*, 8906.
- Stein, C. A.; Subasinghe, C.; Shinozuka, K.; Cohen, J. S. *Nucleic Acids Res.* **1988**, *16*, 3209.
- Clark, C. L.; Cecil, P. K.; Singh, D.; Gray, D. M. *Nucleic Acids Res.* **1997**, *25*, 4098.
- Xodo, L.; Alunni-Fabbroni, M.; Manzini, G.; Quadrioglio, F. *Nucleic Acids Res.* **1994**, *22*, 3322.
- Kim, S.-G.; Tsukahara, S.; Yokoyama, S.; Takaku, H. *FEBS Lett.* **1992**, *314*, 29.
- Haginoya, N.; Ono, A.; Nomura, Y.; Ueno, Y.; Matsuda, A. *Bioconjugate Chem.* **1997**, *8*, 271.
- Ueno, Y.; Mikawa, M.; Matsuda, A. *Bioconjugate Chem.* **1998**, *9*, 33.
- Matsukura, M.; Okamoto, T.; Miike, T.; Sawai, H.; Shinozuka, K. *Biochem. Biophys. Res. Commun.* **2002**, *293*, 1341.
- Moriguchi, T.; Sakai, H.; Suzuki, H.; Shinozuka, K. *Chem. Pharm. Bull.* **2008**, *56*, 1259.
- Lin, K.-Y.; Jones, R. J.; Matteucci, M. J. *Am. Chem. Soc.* **1995**, *117*, 3873.
- Lin, K.-Y.; Matteucci, M. D. J. *Am. Chem. Soc.* **1998**, *120*, 8531.
- Venkateswaran, S.; Vijayanathan, V.; Shirahata, A.; Thomas, T.; Thomas, T. J. *Biochemistry* **2005**, *44*, 303.
- Winkler, J.; Saadat, K.; Díaz-Gavilán, M.; Urban, E.; Noe, C. R. *Eur. J. Med. Chem.* **2009**, *44*, 670.
- Morvan, F.; Debart, F.; Vasseur, J.-J. *Chem. Biodivers.* **2010**, *7*, 494.
- Michel, T.; Debart, F.; Heitz, F.; Vasseur, J.-J. *ChemBioChem* **2005**, *6*, 1254.
- Fraley, A. W.; Pons, B.; Dalkara, D.; Nullans, G.; Behr, J.-P.; Zuber, G. J. *Am. Chem. Soc.* **2006**, *128*, 10763.
- Fidanza, J. A.; Ozaki, H.; McLaughlin, L. W. J. *Am. Chem. Soc.* **1992**, *114*, 5509.
- Chen, M.; Gothelf, K. V. *Org. Biomol. Chem.* **2008**, *6*, 908.
- The cleavage products were characterized by MALDI-TOF mass data. The alkylation may occur at N7 of guanine residue resulting in cleavage of sugar-base bond.
- The T_m values of the ODNs were summarized in ESI.
- The polypyrimidine ODN was selected so that it also can be used both for duplex and triplex studies.
- Burgers, P. M. J.; Eckstein, F. *Biochemistry* **1979**, *18*, 592.
- Kamisetty, N. K.; Pack, S. P.; Nonogawa, M.; Devarayapalli, K. C.; Watanabe, S.; Kodaki, T.; Makino, K. *Anal. Bioanal. Chem.* **2007**, *387*, 2027.
- Jaroszewski, J. W.; Syi, J.-L.; Maizel, J.; Cohen, J. S. *Anti-Cancer Drug Des.* **1992**, *7*, 253.
- Egli, M.; Portmann, S.; Usman, N. *Biochemistry* **1996**, *35*, 8489.
- Sundaralingam, M.; Pan, B. *Biophys. Chem.* **2002**, *95*, 273.
- Egli, M.; Tereshko, V.; Teplova, M.; Minasov, G.; Joachimiak, A.; Sanishvili, R.; Weeks, C. M.; Miller, R.; Maier, M. A.; An, H.; Cook, D. P.; Manoharan, M. *Biopolymers* **1998**, *48*, 234.
- Ouameur, A. A.; Tajmir-Riahi, H.-A. *J. Biol. Chem.* **2004**, *279*, 42041.
- Hedra, M. E.; Perillo, I. A. J. *Heterocycl. Chem.* **2000**, *37*, 1431.
- Piper, J. R.; Stringfellow, C. R., Jr.; Elliott, R. D.; Johnston, T. P. *J. Med. Chem.* **1969**, *12*, 236.
- McElvain, S. M.; Bannister, L. W. J. *Am. Chem. Soc.* **1954**, *76*, 1126.

Cholesterol-lowering Action of BNA-based Antisense Oligonucleotides Targeting PCSK9 in Atherogenic Diet-induced Hypercholesterolemic Mice

Tsuyoshi Yamamoto^{1,2}, Mariko Harada-Shiba², Moeka Nakatani^{1,2}, Shunsuke Wada^{2,3}, Hidenori Yasuhara^{1,2}, Keisuke Narukawa¹, Kiyomi Sasaki³, Masa-Aki Shibata⁴, Hidetaka Torigoe³, Tetsuji Yamaoka⁵, Takeshi Imanishi⁶ and Satoshi Obika¹

Recent findings in molecular biology implicate the involvement of proprotein convertase subtilisin/kexin type 9 (PCSK9) in low-density lipoprotein receptor (LDLR) protein regulation. The cholesterol-lowering potential of anti-PCSK9 antisense oligonucleotides (AONs) modified with bridged nucleic acids (BNA-AONs) including 2',4'-BNA (also called as locked nucleic acid (LNA)) and 2',4'-BNA^{NC} chemistries were demonstrated both *in vitro* and *in vivo*. An *in vitro* transfection study revealed that all of the BNA-AONs induce dose-dependent reductions in PCSK9 messenger RNA (mRNA) levels concomitantly with increases in LDLR protein levels. BNA-AONs were administered to atherogenic diet-fed C57BL/6J mice twice weekly for 6 weeks; 2',4'-BNA-AON that targeted murine PCSK9 induced a dose-dependent reduction in hepatic PCSK9 mRNA and LDL cholesterol (LDL-C); the 43% reduction of serum LDL-C was achieved at a dose of 20 mg/kg/injection with only moderate increases in toxicological indicators. In addition, the serum high-density lipoprotein cholesterol (HDL-C) levels increased. These results support antisense inhibition of PCSK9 as a potential therapeutic approach. When compared with 2',4'-BNA-AON, 2',4'-BNA^{NC}-AON showed an earlier LDL-C-lowering effect and was more tolerable in mice. Our results validate the optimization of 2',4'-BNA^{NC}-based anti-PCSK9 antisense molecules to produce a promising therapeutic agent for the treatment of hypercholesterolemia.

Molecular Therapy–Nucleic Acids (2012) 1, e22; doi:10.1038/mtna.2012.16; published online 15 May 2012

Introduction

Statins are lipid-lowering drugs that achieve a strong reduction of serum low-density lipoprotein cholesterol (LDL-C) mainly *via* the indirect activation of LDL receptor (LDLR)-mediated hepatic uptake of LDL from the blood.^{1,2} The development of drugs that directly regulate the expression of hepatic LDLR would thus be a compelling strategy to obtain the efficacy of statin-induced LDL-C reduction while compensating for potential weaknesses of statin therapy, such as severe adverse effects (e.g., myopathy). The molecular basis of LDLR regulation as well as cholesterol maintenance has been enthusiastically elucidated,^{2–7} and several causative molecules of hypercholesterolemia relevant to the direct regulation of LDLR function have recently been identified.^{8–11} Proprotein convertase subtilisin/kexin type 9 (PCSK9), which was recently identified as the third gene relevant to autosomal dominant hypercholesterolemia,¹⁰ is involved in the maintenance of cholesterol balance. A number of human mutations in PCSK9 have been reported. Gain-of-function mutations are associated with autosomal dominant hypercholesterolemia, whereas loss-of-function mutations are relevant to low blood levels of LDL-C.¹² Recent findings have suggested the involvement of PCSK9 in LDLR regulation. PCSK9 is synthesized mainly in the liver, small intestine, and kidney as a 72-kDa soluble zymogen that subsequently undergoes autocatalytic cleavage into an active form. The active 63-kDa

enzyme in complex with the cleaved prodomain is secreted into the bloodstream. Secreted PCSK9 directly binds to an extracellular part of the LDLR. The LDLR–PCSK9 complex is transported from the cell surface to the endosomal system for digestion. PCSK9 forms a stable complex with LDLR in lysosomes, which disturbs the recycling of LDLR to reduce LDL uptake.^{4,13,14} PCSK9 would be a pivotal regulator of LDLR and an attractive target for lipid-lowering therapy, although some molecular functions of PCSK9 remain unknown.

To achieve PCSK9 inhibition, several “molecular-targeted” approaches have been attempted. To our knowledge, berberine, an isoquinoline plant alkaloid, is the sole small molecule that achieves suppression of PCSK9 expression at the transcriptional level.^{15–17} An antibody against secreted PCSK9 efficiently reduced the serum LDL-C levels of mice and monkeys.¹⁸ Small interfering RNA formulated in a lipidoid nanoparticle can induce liver-specific reduction of PCSK9 messenger RNA (mRNA) and serum total cholesterol levels in wild-type mice.¹⁹ These proof-of-concept studies demonstrate the therapeutic promise of PCSK9-targeted therapies. Antisense inhibition of PCSK9 is superior to the aforementioned strategies because antisense oligonucleotide (AON) molecules can deactivate intrahepatic mRNA as well as proteins in the blood; in addition, they target the liver *via* a simple delivery methodology. Graham *et al.* showed that 2'-O-methoxyethyl-modified phosphorothioate oligonucleotide (MOE) (100 mg/kg/week) administered for a 6-week period to mice fed a high-fat diet reduced hepatic

¹Graduate School of Pharmaceutical Sciences, Osaka University, Suita, Japan; ²Department of Molecular Innovation in Lipidology, National Cerebral and Cardiovascular Center Research Institute, Suita, Japan; ³Faculty of Science, Tokyo University of Science, Shinjuku-ku, Japan; ⁴Faculty of Health Science, Osaka Health Science University, Osaka, Japan; ⁵Department of Biomedical Engineering, National Cerebral and Cardiovascular Center Research Institute, Suita, Japan; ⁶BNA Inc., Ibaraki, Japan
Correspondence: Satoshi Obika, 1-6 Yamadaoka, Suita, Osaka 565-0871, Japan. E-mail: obika@phs.osaka-u.ac.jp or Mariko Harada-Shiba, 5-7-1 Fujishirodai, Suita, Osaka 565-8565, Japan. E-mail: shiba.mariko.ri@mail.ncvc.go.jp

Received 6 November 2011; revised 10 April 2012; accepted 10 April 2012

Keywords: antisense; BNA; hypercholesterolemia; LNA; PCSK9

PCSK9 mRNA and serum LDL-C. However, a large dose of MOE is necessary to obtain sufficient efficacy. More recently, Gupta *et al.* demonstrated that a reduced amount of 2',4'-bridged nucleic acid (BNA) (also called as locked nucleic acid (LNA))-modified gapmer efficiently suppresses PCSK9 mRNA and induces an increase in LDLR protein levels both *in vitro* and *in vivo*.²⁰ Due to the high-affinity binding of 2',4'-BNA-modified AON molecules, in many cases, 2',4'-BNA-modified gapmer shows improved antisense potency *in vivo* as compared to MOE-based gapmer. However, in some cases, the repeated administration of 2',4'-BNA-modified gapmer causes hepatotoxicity.²¹ The development of more potent and less toxic antisense molecules is necessary for clinical usage.²² We have developed a series of 2',4'-BNAs such as 2',4'-BNA and 2',4'-BNA^{NC}, which have chemical bridges between the 2' and 4' positions of the ribose rings; 2',4'-BNA^{NC}-modified oligonucleotides retain high-affinity binding to RNA and higher nucleic acid stability than 2',4'-BNA-modified oligonucleotides.²³⁻²⁵ Therefore, 2',4'-BNA^{NC}-modified anti-PCSK9 AONs would be expected to possess distinct cholesterol-lowering potency and toxicological risks *in vivo*. Actually, 2',4'-BNA^{NC}-modified phosphatase and tensin homolog deleted from chromosome ten (PTEN) inhibitor showed high potency without the onset of hepatotoxicity.²⁶ In this study, we present the effective gene silencing and cholesterol-lowering effects of both 2',4'-BNA- and 2',4'-BNA^{NC}-based anti-PCSK9 AON. In addition, we showed the toxicological characteristics of 2',4'-BNA- and 2',4'-BNA^{NC}-based AONs.

Results

Physicochemical properties of a 2',4'-BNA-modified anti-PCSK9 AON *in vitro*

The 2',4'-BNA-modified phosphorothioate oligonucleotides (P900SL) and a conventional phosphorothioate AON (P900S) were designed based on the previously identified potential sequence.²⁷ The control sequence was CR01S, which has the same conventional phosphorothioate backbone as P900S, but does not target any specific genes in mice (Table 1). Upper and lower case letters in the sequences represent 2',4'-BNA and DNA, respectively. We additionally selected another sequence, a consensus sequence between the mouse and human sequences to dispense with the sequence translation to adapt to human clinical trials. P901SL and P901SNC both possess five gaps, and nine of 20 nucleotides are substituted by 2',4'-BNA and 2',4'-BNA^{NC} (Table 1, Figure 1). Note that the sequence, length, and composition of AONs have not been fully optimized yet here. The melting temperature (T_m) values of P900S, P900SL, P901S, P901SL, and P901SNC with their target RNA were determined by UV-melting experiments. AONs modified with 2',4'-BNA and 2',4'-BNA^{NC} showed an excellent target affinity compared to conventional phosphorothioate AONs (Table 1).

In vitro gene silencing properties

We next evaluated *in vitro* gene silencing properties of AONs by using mice hepatic NMuLi cells (Figure 2a-c) treated with 1–50 nmol/l of P900SL by means of lipofection. Real-time reverse transcription-PCR revealed a dose-dependent

Table 1 Properties of modified oligonucleotides used in this study

Sequence ID	Sequencea	T_m	IC ₅₀ (nmol/l)	
			NMuLi	HepG2
CR01S	5'-ccttccctgaaggtcctcc-3'	–	N.D.	–
CR01SL	5'-cctTCCctgaagGTTCCtCCc-3'	–	N.D.	–
P900S	5'-gggctcatagcacattatcc-3'	37.0	23	–
P900SL	5'-GggCTCatagcaCaTtTaTcC-3'	72.1	1.8	–
P901S	5'-ccaggcctatgagggcgccg-3'	49.6	–	100
P901SL	5'-CCaggCCTaTgagggTgCCg-3'	83.2	1.0	1.8
P901SNC	5'-CCaggCCTaTgagggTgCCg-3'	86.0	3.0	11.6

Abbreviations: BNA, bridged nucleic acid; IC₅₀, half-maximal inhibitory concentration.

^aOligonucleotides with 2',4'-BNA (upper case), 2',4'-BNA^{NC} (capital italic), and DNA (lower case letters). All internucleotide linkages are phosphorothioated. Melting temperature (T_m) of CR01S and CR01SL were not measured because no target site on transcripts, marked "–". Non-detectable IC₅₀ values, due to low potency, marked "N.D.". IC₅₀ values were partly not determined, marked "–".

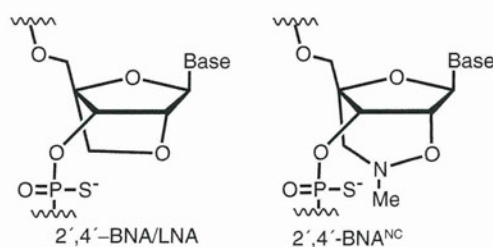


Figure 1 Structure of bridged nucleic acids (BNA) used in this study. LNA, locked nucleic acid.

reduction of the PCSK9 mRNA level as compared to the GAPDH mRNA level (half-maximal inhibitory concentration (IC₅₀) = 3.0 nmol/l) (Figure 2a). By contrast, no such effective reduction of the mRNA level occurred in P900S-treated cells (IC₅₀ = 41.2 nmol/l) (Figure 2a), and treatment with CR01S and CR01SL did not yield any silencing (Figure 2b). To investigate whether suppression of PCSK9 mRNA by P900SL affects the PCSK9 protein level, we performed western blotting experiments. A dose-dependent reduction of the PCSK9 protein level occurred in P900SL-treated NMuLi cells (Figure 2a). On the other hand, the protein levels of LDLR in P900SL-treated cells were increased in a dose-dependent manner, showing the inverse relationship between PCSK9 and LDLR protein levels. PCSK9 protein was thoroughly inhibited by P900SL at a concentration of ~10 nmol/l. The increase in LDLR protein simultaneously reached a plateau at this concentration. Gene silencing properties of P901S, P901SL, and P901SNC were demonstrated both in murine and human hepatic cell lines. P901SL and P901SNC showed a similar silencing efficacy as P900SL in NMuLi cells (Figure 2a). Both P901SL and P901SNC showed far more efficient mRNA inhibitory activity than P901S in HepG2 cells (Figure 2d). The reduction rate of PCSK9 protein levels also supported this trend (Figure 2e).

The level of intrahepatic AONs in normal chow-fed mice after a single treatment with BNA-modified AONs

Next, we examined whether BNA-modified AONs can also be good inhibitors of PCSK9 in mice. A naked AON (P900SL) was intravenously (i.v.), subcutaneously (s.c.), and

intraperitoneally (i.p.) injected into normal chow-fed C57BL/6J mice (**Figure 3**). After 72 hours, the hepatic PCSK9 mRNA levels were measured, and the half-maximal effective dose (ED₅₀) values were determined. Intravenous administration showed the most efficient hepatic reduction of PCSK9 mRNA (ED₅₀ = 7.5 mg/kg) (**Figure 3a**). Subcutaneous and intraperitoneal injections resulted in ED₅₀ values of 8.8 and 12.1 mg/kg, respectively (**Figure 3c,d**). Next, we measured the amount of intact P900SL that accumulated in the liver after i.v. administration by using a previously described ELISA method.²⁸ The intrahepatic content of P900SL was directly proportional to the applied doses, and the saturation of accumulation was not observed even at the highest dose of 70 mg/kg, which is consistent with a previous report²⁹ (**Figure 3b**).

Repeated administration of BNA-modified AONs to atherogenic diet-fed mice

To determine the pharmacological effects of BNA-modified AONs, we monitored the serum cholesterol change upon repeated administration of AONs. Naked AONs (P900S and P900SL) were i.p. injected into atherogenic diet (cholesterol content, 1.25%)-fed C57BL/6J mice twice during 5 days at a dosage of 10 mg/kg per administration. Injections were performed on days 1 and 4. On day 5, livers were harvested to measure gene expression, and blood was collected for the lipid component analysis and toxicity evaluation. As shown in **Figure 4a**, a significant silencing effect of the hepatic PCSK9 mRNA level was only observed in the P900SL-treated arm. The increase in hepatic LDLR protein was shown by western blotting analysis (**Figure 4c**). The average serum LDL-C levels were concomitantly reduced by ~30%, although no statistically significant differences were observed (**Figure 4b**). Collectively, P900SL showed a mild cholesterol-lowering effect in this short-term experiment with the lack of serum elevation of liver transaminases, aspartate aminotransferase and alanine aminotransferase (ALT) (**Figure 4d**).

To obtain cholesterol-lowering efficacy profiles and toxicological information, we next performed longer-term and multiple-dose experiments in mice. P900SL was i.p. injected twice weekly at a dosage of 2–40 mg/kg/week for 6 weeks into high-cholesterol-loaded mice. After 4 weeks of treatment, blood samples were collected from tail veins, and the precise cholesterol profiles in serum lipoproteins were analyzed by the high-performance liquid chromatography method. **Supplementary Table S1** shows the raw serum total cholesterol levels and the cholesterol levels of fractionated lipoprotein components. **Figure 5a,b** show raw data plots of the high-performance liquid chromatography analysis of serum and the serum LDL-C ratio. Total cholesterol levels did not show a cholesterol-lowering effect or any other specific trends with an increase of doses. However, a precise lipoprotein component analysis revealed that P900SL had induced a dose-dependent LDL-C reduction, and the serum LDL-C reduction of 43% was achieved at a dose of 40 mg/kg/week, whereas serum HDL-C levels increased inversely with LDL-C levels. After a 6-week dosing regimen, livers and blood were harvested to analyze gene and protein expression and toxicities. A dose-dependent decrease of LDL-C, as seen at week 4, was continuously observed. Intrahepatic cholesterol content showed no significant difference between arms

(**Supplementary Figure S1 and Supplementary Materials and Methods**). Hepatic gene expression levels were analyzed by the real-time reverse transcription-PCR method. Hepatic PCSK9 mRNA was efficiently reduced in a dose-dependent manner (**Figure 5c**). And, the reduction of PCSK9 mRNA did not affect LDLR mRNA expression levels (**Figure 5e**). However, LDLR protein levels increased concomitantly with decreased LDL-C levels (**Figure 5d**). Hepatic LDLR protein levels were significantly increased by ~1.5-fold in a dose-dependent manner. Note that we here collected sera and analyzed lipid profiles 2 weeks ahead of sacrifice in order to distribute the stressors associated with treatments, which strongly disturbs serum cholesterol levels.

Related gene expression associated with repeated dosing

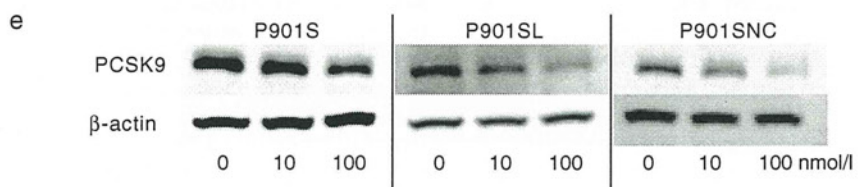
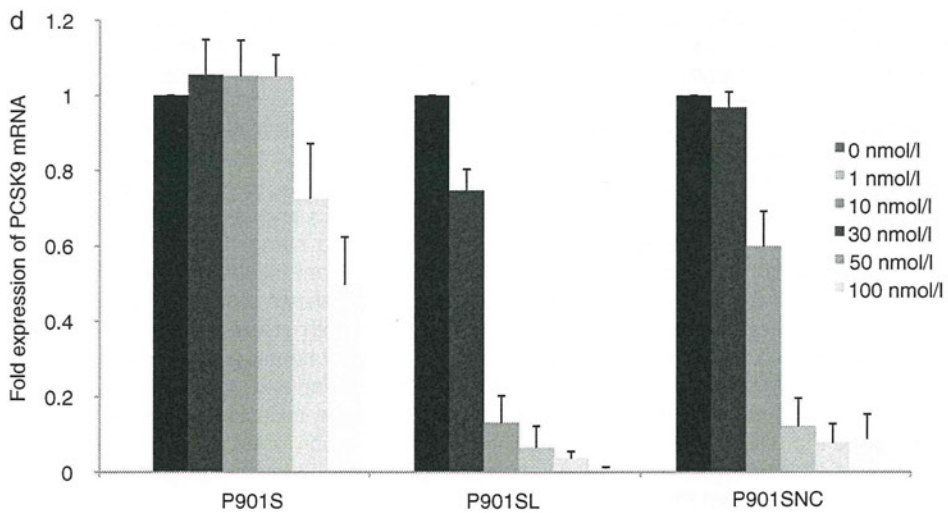
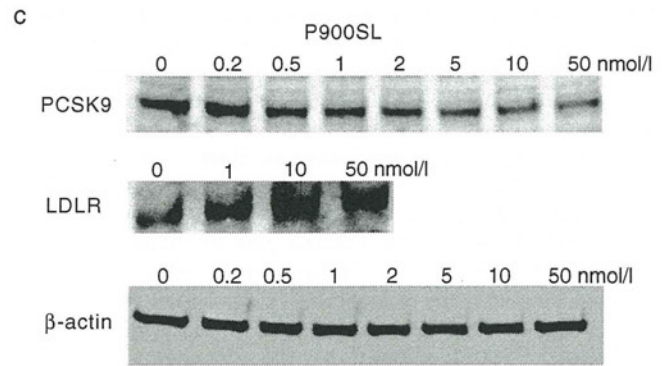
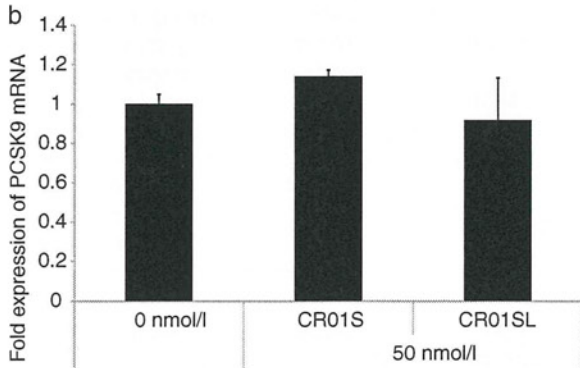
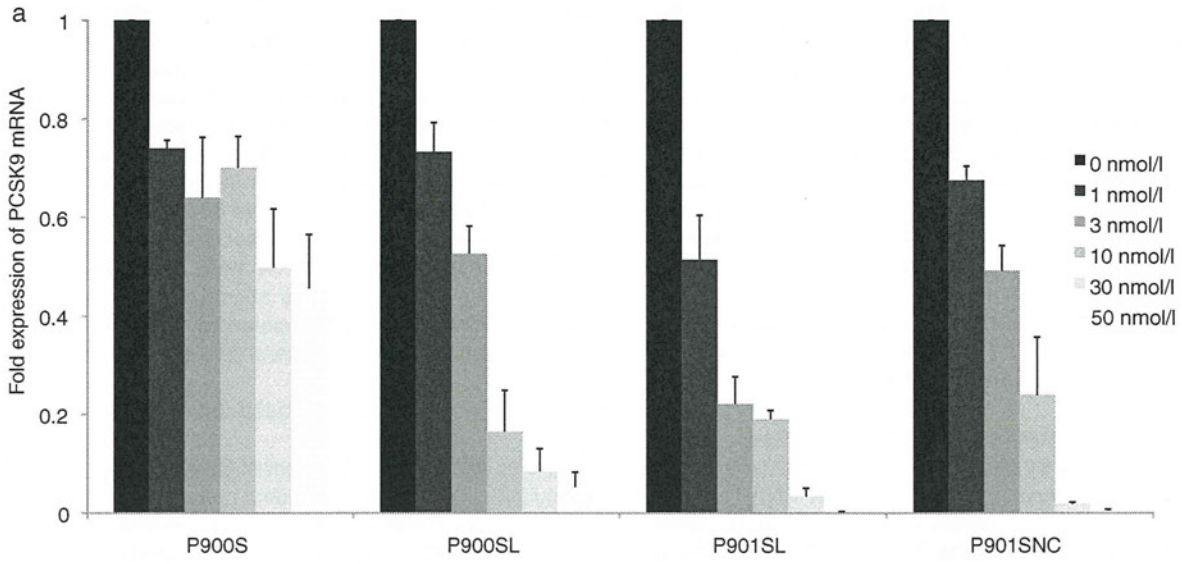
We further investigated the effect of BNA-modified AONs on molecules related to the cholesterol metabolism (**Figure 5e**). Knockdown of PCSK9 mRNA induced a reduction in the gene expression of sterol regulatory element-binding protein 2 (SREBP2), a transcriptional factor controlling sterol synthesis; hydroxymethylglutaryl-CoA (HMG-CoA) synthase, an enzyme in the cholesterol synthesis pathway; hepatic triglyceride lipase (LIPC); and ATP-binding cassette transporter (ABCA1), a key enzyme for HDL production. On the other hand, scavenger receptor class B type 1 (SR-B1), a receptor for HDL particles, and cholesterol acyltransferase (ACAT1) showed no significant change, and the expression level of cholesterol 7 α -hydroxylase (CYP7A1), the first and rate-limiting enzyme in bile acid synthesis, dose-dependently increased.

Toxicological characteristics of BNA-AONs associated with repeated dosing

Toxicological characteristics of P900SL upon subchronic dosing were estimated by an analysis of blood biochemistry and a histopathological analysis (**Figure 6**). Because phosphorothioate AONs accumulate mainly in the kidney and liver,^{30–32} hepatotoxicity and renal toxicity are the most likely types of toxicity; 2',4'-BNA-based AONs have the potential to induce hepatotoxicity.²¹ However, our experiments showed only moderate increases in liver transaminases (even at higher doses of P900SL) and a dose-dependent mild increase in serum blood urea nitrogen levels (**Figure 6a**). Histopathologically, no treatment-related changes were seen in the liver or kidneys. As shown in **Figure 6b**, although the majority of mice treated with saline or therapeutic regimes showed cloudy swelling of hepatocytes, no cellular damage was found in the centrilobular and perilobular hepatocytes, which frequently experience toxicological insults. In addition, granulomas or inflammation were sporadically observed in the saline group and treated groups (**Supplementary Table S2**).

Repeated administration of 2',4'-BNA^{NC}-modified AONs to atherogenic diet-fed mice with the least toxicity

To examine the effect of 2',4'-BNA^{NC}-modified AONs, P901SNC as well as P901SL were applied to atherogenic diet-fed mice to investigate their potencies and toxicity profiles. P901SL and P901SNC were i.p. administered twice weekly for 6 weeks at a dose of 1–20 and 1–10 mg/kg/injection, respectively. On week 4, peripheral blood was collected from tail veins, and



the cholesterol content of each lipoprotein fraction was measured. P901SL showed no significant reduction of LDL-C levels, whereas P901SNC reduced serum LDL-C levels by ~30% at the highest dose (10 mg/kg/injection), and the reduction occurred in a dose-dependent manner (**Figure 7a**). We observed a slower onset of the reduction of LDL-C of P901SL 6 weeks after the first treatment (**Supplementary Figure S2**). Meanwhile, hepatic PCSK9 mRNA expression was suppressed and the hepatic LDLR protein was increased accompanied by AON treatment with relatively large deviations (**Figure 7b,c**). PCSK9 mRNA was inhibited by P901SL and P901SNC as efficiently as P900SL. LDLR protein responded maximally to 20 mg/kg/injection of P901SL and 10 mg/kg/injection of P901SNC. The increasing rates of these two arms were nearly the same (~1.5-fold increase). The lack of severe hepatotoxicities or kidney toxicities was confirmed by serum chemistry in both the P901SL- and P901SNC-treated arms (**Supplementary Table S3**). Collectively, 2',4'-BNA^{NC}-based AON, P901SNC, was as safe as the 2',4'-BNA-based counterpart, P901SL.

Discussion

We demonstrated in this article that BNA-based antisense therapeutics successfully inhibited hepatic PCSK9 expression, resulting in a strong reduction of the serum LDL-C levels of mice. Our findings support the hypothesis that PCSK9 is a potential therapeutic target for hypercholesterolemia. To the best of our knowledge, this is the first time that we were able to show that BNA-based AONs induced cholesterol-lowering action in hypercholesterolemic mice. P900SL yielded high inhibitory activity *in vivo* as well as *in vitro*, and *i.v.* administration gave the highest peak inhibitory activity of the three representative routes. Nevertheless, *i.p.* and *s.c.* injections are alternative routes to *i.v.* injection, because they yielded adequate dose-responsive suppression of PCSK9 mRNA. In fact, Mipomersen for the treatment of hypercholesterolemia is given *s.c.* rather than *i.p.* due to practicality.^{33,34} The rationality of *s.c.* injection is also supported by the pharmacokinetic nature and disposition properties of 2'-O-methyl phosphorothioate AON.³⁵ The peak tissue levels of 2'-O-methyl phosphorothioate AON after *i.v.* injection were higher than after *s.c.* and *i.p.* administration, and *i.v.* injection gives the peak of exon skipping efficiency. However, the bioavailability of 2'-O-methyl phosphorothioate AON was similar among all routes, and durable effects were observed after *s.c.* administration; therefore, the investigators selected *s.c.* administration for a preclinical study in mice. On the other hand, the hepatic accumulation of P900SL associated with a single *i.v.* injection increased directly with dose. This result was totally consistent with a 2',4'-BNA gapmer targeting apolipoprotein B.²⁹ Further research to elucidate the pharmacokinetics of BNA-AONs is now underway.

The *in vivo* silencing properties of 2',4'-BNA-based AON that targets PCSK9 mRNA were previously reported by Gupta

*et al.*²⁰ They achieved the silencing of PCSK9 concomitantly with the upregulation of hepatic LDLR in female mice. However, they did not mention the cholesterol-lowering effect of the 2',4'-BNA-based AON. We observed a dose-dependent decrease of LDL-C levels and a dose-dependent increase of HDL-C levels (**Figure 5**). There seems to be no trend in the net changes of serum total cholesterol levels (**Supplementary Table S1**). The increase in LDLR protein levels reported by Gupta *et al.*²⁰ were a little higher than those in **Figure 5d**. The likely explanation is the difference of experimental conditions in which they have used female NMRI mice with standard maintenance diet, whereas we used male C57BL/6J mice with atherogenic diet which contains 1.25% of cholesterol, 0.5% of cholic acid, and so on. Hepatic influx of these ingredients in the diet are known to strongly induce the downregulation of LDLR and cholesterol biosynthetic enzymes such as HMG-CoA reductase by downregulating SREBPs, important transcriptional factors, which results in LDLR reduction.^{13,36,37} We also observed dose-dependent moderate increases of aspartate aminotransferase, ALT, and blood urea nitrogen levels, whereas histopathological analysis revealed no severe hepatic toxicities (**Figure 6, Supplementary Table S2**). Collectively, a continuous dosing of P900SL showed potent LDL-C reduction in mice without severe side effects, and this report provides the experimental proof of the cholesterol-lowering effects of BNA-based AONs.

We also achieved a dose-dependent decrease in serum LDL-C levels by using a 2',4'-BNA^{NC}-based AON (P901SNC) (**Figure 7a**). In this case, serum HDL-C levels and the levels of liver and kidney toxicity indicators were not elevated (**Supplementary Table S3**). When compared with P901SNC, a delayed decrease of LDL-C levels was observed in the P901SL-treated arm (**Supplementary Figure S2**). We also showed here that a 2',4'-BNA^{NC}-based AON (P901SNC) has greater potential to inhibit PCSK9 and to reduce serum cholesterol levels with no toxicity than a conventional 2',4'-BNA-based AON. The high-potency and low-toxicity characteristics of a 2',4'-BNA^{NC}-based AON were previously reported to effectively inhibit PTEN mRNA without elevation of the serum ALT level, whereas elevated serum ALT was observed in the 2',4'-BNA counterpart-treated arm.²⁶ Thus, we conclude that 2',4'-BNA^{NC}-based AONs can be a promising therapeutic agent for antisense therapy. However, the structure-activity relationship of BNA-based AONs still remains to be elucidated.

As previously reported, LDLR mRNA expression was independent of PCSK9 inhibition.^{20,27} The coordinate repression of SREBP2, HMG-CoA synthase, and ABCA1 is in agreement with a response to a transient massive influx of cholesterol in the liver (**Figure 5e**). HMG-CoA synthase and ABCA1 are both known to be regulated by SREBP2, whereas SR-B1 and ACAT1 are atypical factors regulated by SREBP2.³⁴ The mRNA expression levels of the latter two factors were unchanged by P900SL, while an increased expression level of CYP7A1 was induced by P900SL. CYP7A1 is the first and

Figure 2 *In vitro* silencing properties of AONs (CR01S, CR01SL, P900S, P900SL, P901SL, and P901SNC). AONs were transfected into NMuLi cells. (a,b) After a 24-hour incubation, cells were collected and the expression levels of PCSK9 mRNA were determined. Data represent means ± SD. (c) PCSK9 and LDLR proteins were also detected by western blotting. AONs (P901S, P901SL, and P901SNC) were transfected into HepG2 cells. (d) After a 24-hour incubation, HepG2 cells were collected and the expression levels of PCSK9 mRNA were determined. Data represent mean values ± SD. (e) PCSK9 and β-actin proteins were detected by western blotting. AON, antisense oligonucleotide; LDLR, low-density lipoprotein receptor; mRNA, messenger RNA.

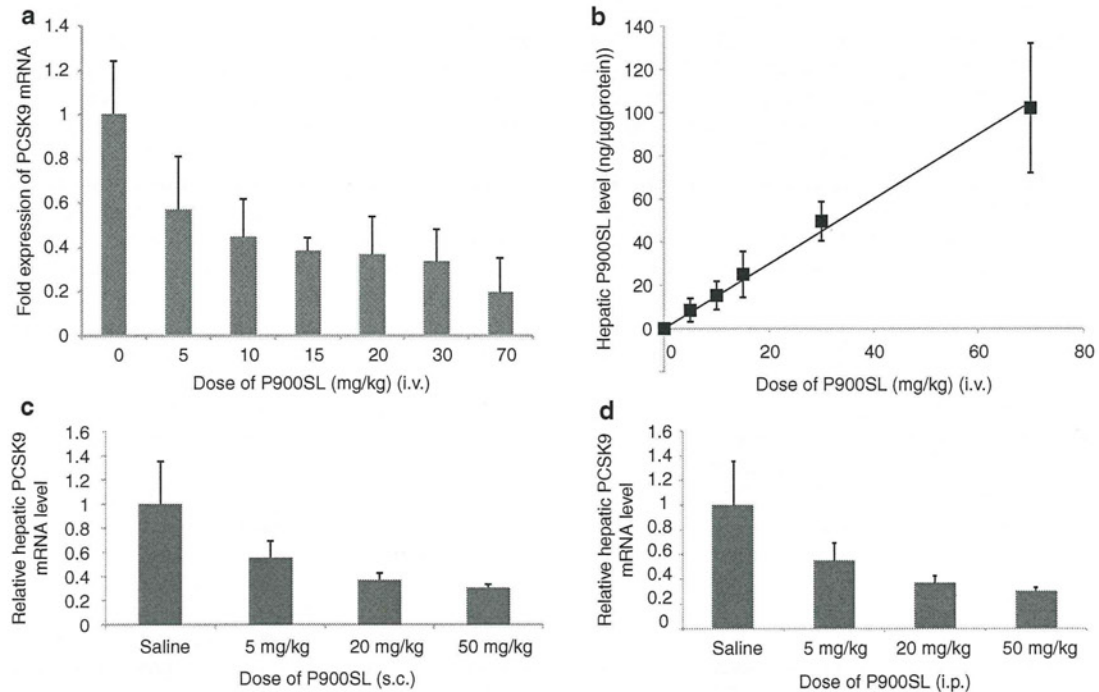


Figure 3 Single administration of P900SL to normal-chow fed C57BL/6J mice. (a,b) Hepatic PCSK9 messenger RNA (mRNA) level and P900SL content 72 hours after a single intravenous (i.v.) administration were expressed as a function of dose level. (c,d) Liver PCSK9 mRNA expression level was measured and presented for each dose 72 hours after subcutaneous (s.c.) and intraperitoneal (i.p.) injection, respectively. Data represent mean values \pm SD. $n = 4-7$.

rate-limiting enzyme in bile acid synthesis; bile acids are versatile signaling molecules that play critical roles in maintaining the homeostasis of cholesterol, lipid, glucose, and energy.^{38,39} CYP7A1 deficiency in humans is associated with dyslipidemia, the formation of gallstones, and atherosclerosis.⁴⁰ A previous report showed that C57BL/6J mice overexpressing CYP7A1 are less susceptible to atherogenic diet-induced elevations of very low-density lipoprotein, intermediate-density lipoprotein, and LDL-C and to reductions of HDL-C and triglyceride and less susceptible to the formation of gallstones and atherosclerosis than their nontransgenic littermates.^{41,42} Similarly, under atherogenic conditions, we observed a reduction in the serum LDL-C level and induction of HDL-C in P900SL-treated mice; these effects may be partly due to the induction of CYP7A1 to maintain intrahepatic cholesterol homeostasis. Collectively, we observed the strong induction of CYP7A1 mRNA associated with the strong suppression of PCSK9. Further investigation of underlying mechanisms of PCSK9 inhibition in atherogenic diet-fed mice are necessary to extrapolate the cholesterol-lowering efficacy of PCSK9 inhibitors in humans.

In conclusion, we found that the strong inhibition of PCSK9 by BNA-based AONs can greatly reduce serum LDL-C levels in atherogenic diet-fed mice via a novel mechanism of CYP7A1 upregulation. These results indicate that PCSK9 is an excellent drug target for the treatment of hypercholesterolemia. Although a structure of AON has not been fully optimized yet here, the 2',4'-BNA^{NC}-based AON shows higher potency than its 2',4'-BNA counterpart and like 2',4'-BNA shows no toxicity under the conditions tested. Meanwhile, a recent report from Gupta *et al.* demonstrated the superiority of a shorter AON

with a smaller number of 2',4'-BNA modifications over a conventional 20-mer 2',4'-BNA-gapmer in an antisense potency. They have used a 13-mer AON with five 2',4'-BNAs and eight gaps that efficiently inhibit the expression of PCSK9 mRNA and protein. We suppose that 2',4'-BNA^{NC}-based AON also has its own unique optimal structure and a further optimization of sequence, length, and composition of 2',4'-BNA^{NC}-based AONs would provide a more reliable 2',4'-BNA^{NC}-based PCSK9 inhibitor.

Materials And Methods

AONs. Two types of modified nucleic acids, 2',4'-BNA and 2',4'-BNA^{NC}, were partially incorporated into 20-mer phosphorothioated oligodeoxyribonucleotides with various sequences. CR01S and CR01SL were 20-mer phosphorothioate DNA and 2',4'-BNA-modified AON, respectively, designed not to target any gene in mice. P900S and P900SL were designed to target murine PCSK9 mRNA, and their sequences have been reported previously. P901S, P901SL, and P901SNC target an identical consensus sequence on mice and human PCSK9 mRNA but have different chemistries. The exact sequences of molecules used in this study are presented in **Table 1**. A large-scale synthesis of 2',4'-BNA^{NC} units was conducted by BNA (Osaka, Japan). All 2',4'-BNA^{NC} monomer units were obtained from BNA. All modified oligonucleotides were provided by Gene Design (<http://www.genedesign.co.jp/>). The syntheses were conducted by standard phosphoramidite procedures, and products were carefully processed under aseptic conditions and purified. All

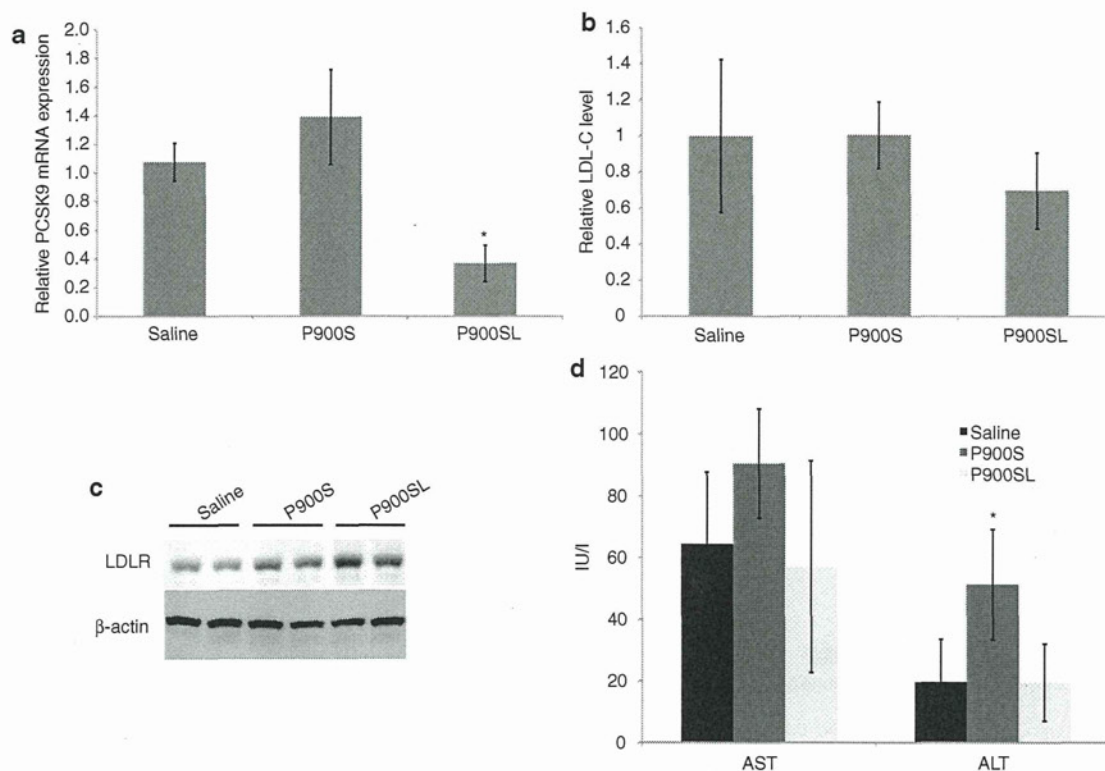


Figure 4 Short-term effects of P900S and P900SL. Atherogenic diet-fed mice received intraperitoneal administration of P900S or P900SL at a dose of 10 mg/kg twice during 4 days. (a) Liver PCSK9 mRNA levels 4 days after the first injection. (b) Relative serum LDL-C levels 4 days after the first injection. (c) Hepatic LDLR protein expression levels were estimated by western blotting. (d) Serum liver transaminases (AST, ALT) were analyzed. Data represent mean values (\pm SD). * $P < 0.05$. ALT, alanine aminotransferase; AST, aspartate aminotransferase; LDL-C, low-density lipoprotein cholesterol; LDLR, low-density lipoprotein receptor; mRNA, messenger RNA.

products were endotoxin-free and contained low levels of residual salts for *in vivo* usage.

In vitro transfection procedures. For AON transfection experiments, NMuLi cells or HepG2 cells were seeded at 5.0×10^5 cells per well in 6-well plates. AONs were transfected by using Lipofectamine 2000 (Invitrogen, Carlsbad, CA) according to the manufacturer's procedures. After a 4-hour transfection, cells were continuously incubated for an additional 20 hours at 37 °C. After incubation, cells were collected and subjected to subsequent analyses.

In vivo pharmacological experiments. All animal procedures were performed in accordance with the guidelines of the Animal Care Ethics Committee of the National Cerebral and Cardiovascular Center Research Institute (Osaka, Japan). All animal studies were approved by an institutional review board. C57BL/6J mice were obtained from CLEA Japan (Tokyo, Japan). All mice were male, and studies were initiated when animals were 6–8 weeks of age. Mice were maintained on a 12-hour light/dark cycle and fed *ad libitum*. Mice were fed a normal chow (CE-2; CLEA Japan) or an artery-hardening food, F2HFD1 (Oriental Yeast, Tokyo, Japan) for 2 weeks before the first treatment and during treatment. Mice received single or multiple treatments of AONs administered *i.v.*, *i.p.* or *s.c.* in the dose range of 1–70 mg/kg/injection. Peripheral blood was collected from a tail vein in BD Microtainers (BD, Franklin Lakes, NJ) for separation of

serum. Lipid component analysis of serum was performed by Skylight Biotech (<http://www.skylight-biotech.com/>). At the time of sacrifice, mice were anesthetized with diethyl ether (Wako, Osaka, Japan). Livers were harvested and snap-frozen until subsequent analysis. Whole blood was collected and subjected to serum separation for subsequent analysis.

mRNA quantification. Total RNA was isolated from cultured cells or mouse liver tissues by using TRIzol Reagent (Invitrogen) according to the manufacturer's procedure. Gene expression was evaluated by a two-step quantitative reverse transcription-PCR method. Reverse-transcription of RNA samples was performed by using a High Capacity cDNA Reverse-Transcription Kit (Applied Biosystems, Foster City, CA), and quantitative PCR was performed by a Fast SYBR Green System or TaqMan Gene Expression Assays (Applied Biosystems). The mRNA levels of target genes were normalized to the GAPDH mRNA level. The following primer sets were used for quantitative PCRs. For murine PCSK9; forward: 5'-TCAGTTCTGCACACCTCCAG-3', reverse: 5'-GGGTAAGGTGCGGTAAGTCC-3' and forward: 5'-GCTCACTG TCAAGGGAAGG-3', reverse: 5'-CGTTGAGGATGCGGCTA TAC-3'. For human PCSK9; forward: 5'-AAGGGAAGGG CACGGTTAG-3', reverse: 5'-GAGTAGAGGCAGGCATCG TC-3'. For murine GAPDH; forward: 5'-GTGTGAACGGATTT GGCCGT-3', reverse: 5'-GACAAGCTTCCCATTCTCGG-3'

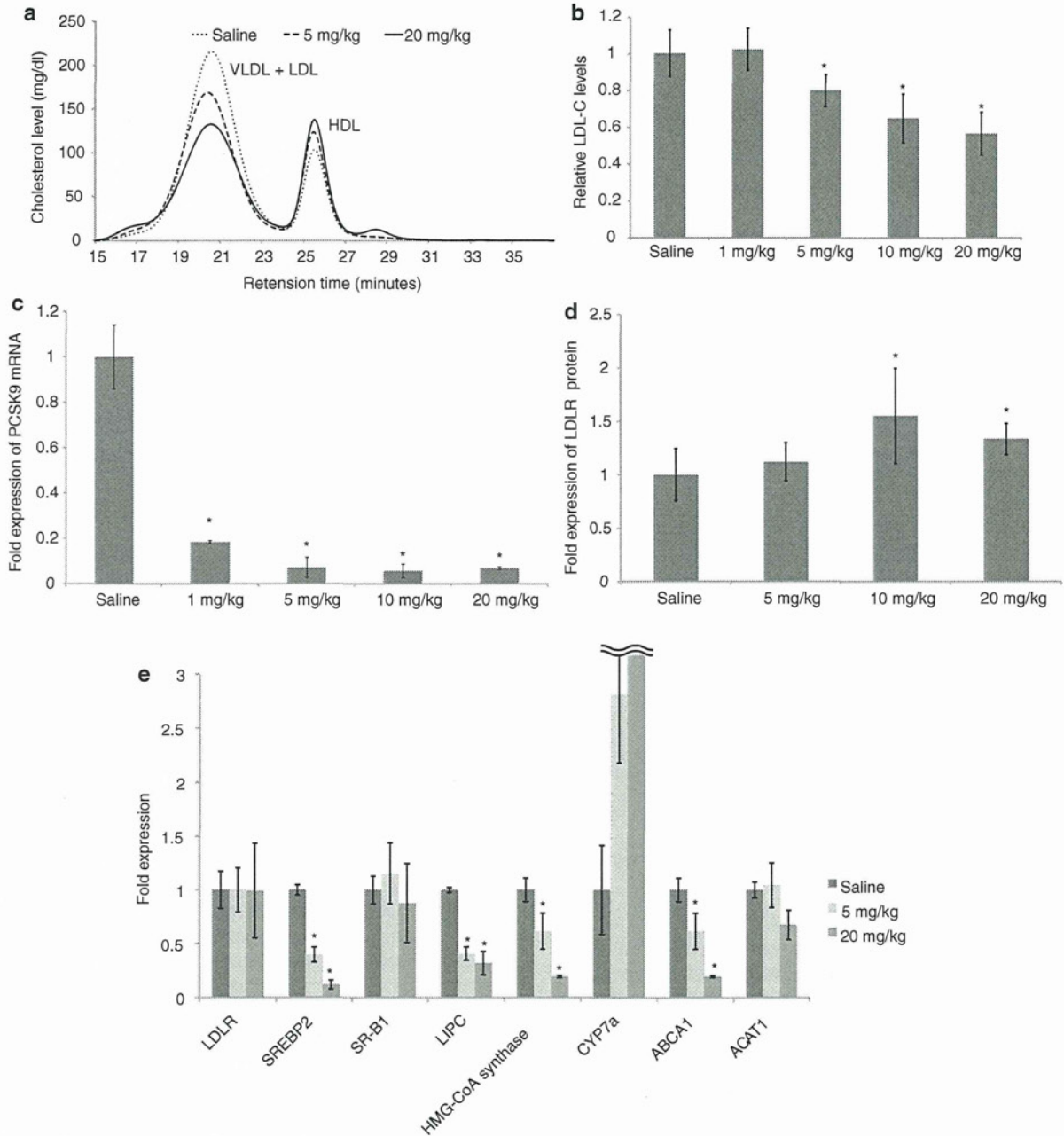


Figure 5 Dose-dependent responses of physiological parameters to P900SL dosing. (a) Changes in cholesterol fractions upon administration of P900SL analyzed by HPLC. (b) Ratio of serum LDL-C levels after 4 weeks of treatment to before treatment were arranged in order of doses. (c) Liver PCSK9 mRNA levels were measured at all dose levels after 6 weeks of treatment. (d) Hepatic LDLR protein levels were determined 6 weeks after treatment started. (e) The expression levels of genes regulating lipid homeostasis in liver were analyzed. Data represent mean values \pm SD. * $P < 0.05$. $n = 5$. HDL, high-density lipoprotein; HPLC, high performance liquid chromatography; LDL, low-density lipoprotein; LDL-C, LDL cholesterol; LDLR, LDL receptor; mRNA, messenger RNA; VLDL, very LDL.

and for human GAPDH; forward: 5'-GAGTCAACGG ATTTGGTTCGT-3', reverse: 5'-GACAAGCTTCCCGTTCTC AG-3'. For murine LDLR, SREBP2, SR-B1, LIPC, HMGCS2, CYP7A1, ABCA1, and ACAT1, TaqMan Gene Expression Assays were used; assay IDs: Mm00440169_m1, Mm01306297_g1, Mm00450236_m1, Mm01147313_m1, Mm00550050_m1, Mm00484152_m1, Mm01350760_m1, Mm00507463_m1, respectively.

Western blotting analysis. Cultured cells and frozen liver tissues were suspended in lysis buffer (150 mmol/l NaCl, 1.0% IGEPAL CA-630, 0.5% sodium deoxycholate, 0.1% SDS, 50 mmol/l Tris, pH 8.0, 20 \times Complete Mini protease inhibitor cocktail 1:20 (Roche, Indianapolis, IN)) and homogenized with TissueLyser II (Qiagen, Valencia, CA). Total protein concentrations were measured with a detergent compatible assay kit (Bio-Rad, Hercules, CA). Solutions were subjected

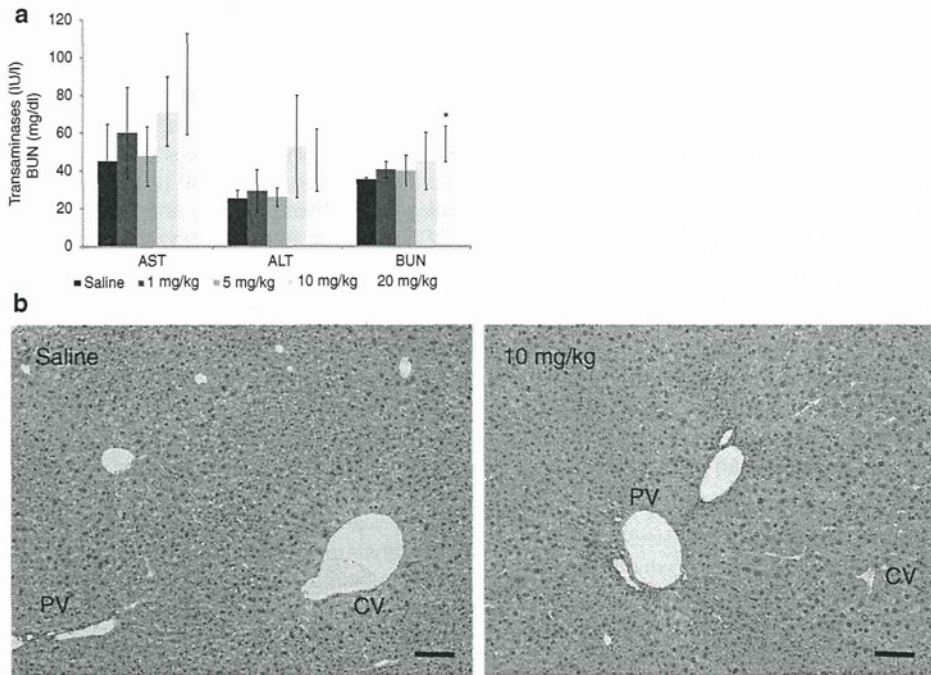


Figure 6 Changes in toxicological parameters upon P900SL dosing. (a) Serum liver transaminases (AST and ALT) and BUN levels were measured. Data represent mean values \pm SD. * $P < 0.05$. (b) Representative H&E stain images of liver of saline- and P900SL-treated mice. Bar indicates 100 μ m. AST, aspartate aminotransferase; ALT, alanine aminotransferase; BUN, blood urea nitrogen; CV, central vein; H&E, hematoxylin and eosin; PV, portal vein.

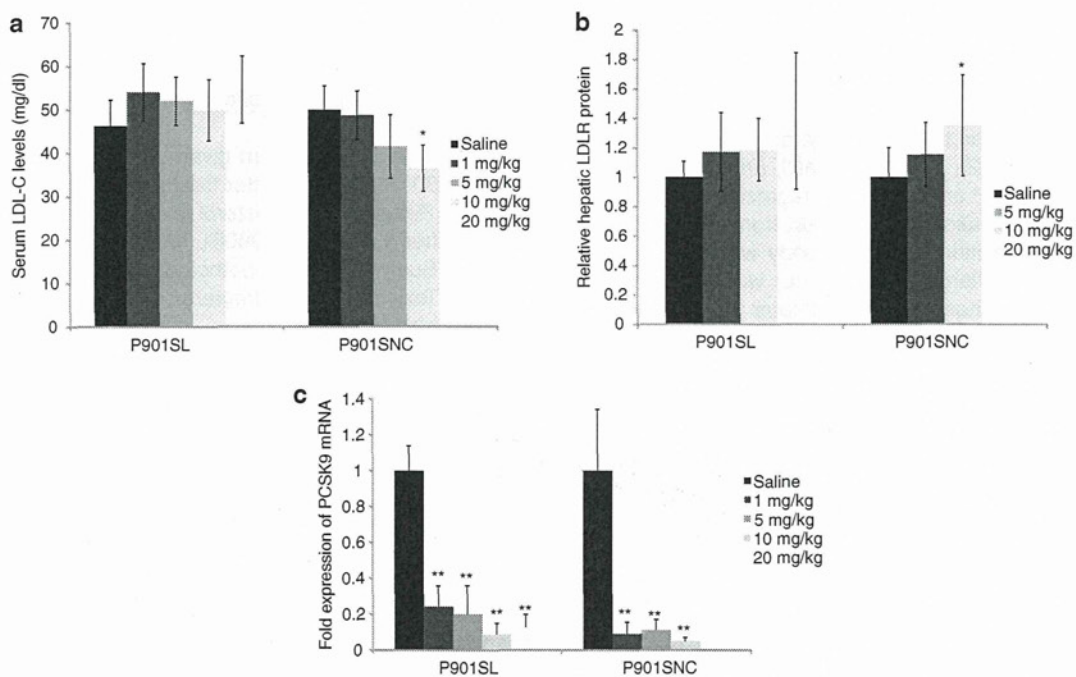


Figure 7 Dose-dependent and chemistry-dependent differences in serum LDL-C levels, hepatic LDLR protein, and PCSK9 mRNA levels after treatment of P901SL and P901SNC. (a) Raw values of serum LDL-C were obtained at 4th week of schedule. (b) Hepatic LDLR protein expression levels were measured after the end of the schedule. (c) Liver PCSK9 mRNA levels were measured at all dose levels after 6 weeks of treatment. Data represent mean values \pm SD. * $P < 0.05$, ** $P < 0.001$ (versus a saline-treated control arm). $n = 5$. LDL-C, low-density lipoprotein cholesterol; LDLR, low-density lipoprotein receptor; mRNA, messenger RNA.

to electrophoresis on 16 or 6% Tris-glycine gels (Invitrogen) and transferred to a polyvinylidene difluoride membrane (Bio-Rad). PCSK9 western blotting was performed at room temperature for 1 hour with a primary anti-rabbit PCSK9 antibody (1:200; Abcam, Cambridge, UK). Additional analyses were performed by using anti-LDLR antibody (R&D Systems, Minneapolis, MN) and anti- β actin antibody (Cell Signaling Technology, Danvers, MA). Membranes were washed three times with phosphate-buffered saline containing 0.3% Tween 20. Blots were labeled by using horseradish peroxidase-conjugated secondary antibodies, either goat anti-rabbit or donkey anti-goat antibodies (Santa Cruz Biotechnology, Santa Cruz, CA). Chemiluminescent detection was performed by using an ECL plus Western blot detection kit (Amersham Biosciences, Buckinghamshire, UK), and bands were visualized by using an LAS-4000mini image analyzer (Fuji Film, Tokyo, Japan). β -Actin expression levels were used as an internal standard.

The determination of P900SL content in liver

Materials and reagents. The template DNA was a 29-mer DNA (5'-gaatagcggagataatgtgctatgagccc-3'), which is complementary to P900SL, with biotin at the 3'-end. The ligation probe DNA was a 9-mer DNA (5'-tcgctattc-3') with phosphate at the 5'-end and digoxigenin at the 3'-end. The template DNA and the ligation probe DNA were purchased from Japan Bio Services (Saitama, Japan). Reacti-Bind NeutrAvidin-coated polystyrene strip plates were purchased from Thermo Fisher Scientific (Waltham, MA) (nunc immobilizer streptavidin F96 white, 436015). The template DNA solution (100 nmol/l) was prepared in hybridization buffer containing 60 mmol/l Na_2HPO_4 (pH 7.4), 0.9 mol/l NaCl, and 0.24% Tween 20. The ligation probe DNA solution (200 nmol/l) was prepared in 1.5 units/well of T4 DNA ligase (TaKaRa, Shiga, Japan) with 66 mmol/l Tris-HCl (pH 7.6), 6.6 mmol/l MgCl_2 , 10 mmol/l DTT, and 0.1 mmol/l ATP.

The washing buffer used throughout the assay contained 25 mmol/l Tris-HCl (pH 7.2), 0.15 mol/l NaCl, and 0.1% Tween 20. Anti-digoxigenin-AP antibody (Fab fragments conjugated with alkaline phosphatase) was obtained from Roche Diagnostics. A 1:2,000 dilution of the antibody with 1:10 super block buffer in TBS (Pierce, Rockford, IL) was used in the assay. The alkaline phosphatase luminous substrate was prepared in 250 $\mu\text{mol/l}$ CDP-Star (Roche) with 100 mmol/l Tris-HCl (pH 7.6) and 100 mmol/l NaCl.

Sample preparation. Frozen liver tissue was collected in a 2-ml tube with 1 ml of phosphate-buffered saline and a zirconia ball (ϕ 5 mm; Irie, Tokyo, Japan) and mechanically homogenized for 2 minutes at 30 oscillations per second by a TissueLyser II apparatus (Qiagen). Total protein concentrations were measured with a detergent compatible assay kit (Bio-Rad) and adjusted to 8 mg/l with phosphate-buffered saline. The assay was performed at the concentration range of 128 pmol/l–400 nmol/l in duplicate. For the standard curve, 10 standard solutions were prepared. To AON-untreated mice, liver homogenates were added to P900SL solutions to prepare 10 standard samples at a range of 128 pmol/l–400 nmol/l.

Assay procedures. The template DNA solution (100 μl) and standard solution (10 μl) or liver homogenates (10 μl) containing the P900SL were added to Reacti-Bind NeutrAvidin-coated polystyrene strip 96-well plates and incubated

at 37 °C for 1 hour to allow the binding of biotin to streptavidin-coated wells and hybridization. After hybridization, the plate was washed three times with 200 μl of washing buffer. Then, ligation probe DNA solution (100 μl) was added, and the plate was incubated at room temperature (15 °C) for 3 hours. The plate was then washed three times with the washing buffer. Subsequently, 200 μl of a 1:2,000 dilution of anti-digoxigenin-AP was added, and the plate was incubated at 37 °C for 1 hour. After washing three times with the washing buffer, CDP-Star solution was added to the plate, and finally the luminescence intensity was determined by using a Centro XS³ luminometer (Berthold Technologies, Bad Wildbad, Germany) one second after the addition of CDP-Star. The linear range of 128 pmol/l–400 nmol/l in this ELISA system was determined as $r > 0.99$.

Serum chemistry and hematoxylin and eosin staining. Serum from blood collected from the inferior vena cava upon sacrifice was subjected to serum chemistry. Assay kits (WAKO) were used to measure serum levels of aspartate aminotransferase, ALT, blood urea nitrogen, and creatinine, which are biomarkers for hepatic and kidney toxicities. Formalin-fixed liver samples (20% formalin; WAKO) were sliced by microtome (Leica Microsystems, Wetzlar, Germany), embedded in Histsec (Merck, Darmstadt, Germany) and stained with Carrazzi's hematoxylin and Tissue-Tek eosin solutions.

Statistical analysis. Pharmacological studies were performed with 5–7 mice per treatment group. A Student's *t*-test was performed for comparison of two arms. $P < 0.05$ or $P < 0.01$ was considered to be of statistical significance.

Supplementary Material

Figure S1. Comparison of intrahepatic cholesterol levels between control and 20 mg/kg/injection of P900SL-treated arms.

Figure S2. Relation between given dose and serum LDL-C levels of P901SL 6 weeks after treatment started.

Table S1. Serum raw cholesterol levels in atherogenic diet-fed mice after 4 weeks of P900SL treatment.

Table S2. Summary of histopathological findings.

Table S3. Toxicological parameters.

Materials and Methods.

Acknowledgments. We thank Eiko Shibata, Mai Inoue, Megumu Morimoto, and Manami Sone for their technical support, who are affiliated with National Cerebral and Cardiovascular Center Research Institute. A part of this work was supported by the Program for Promotion of Fundamental Studies in Health Sciences of the National Institute of Biomedical Innovation (NIBIO) and a research grant from the Ministry of Health, Labor, and Welfare (H23-seisakutansaku-ippan-004). T.Y. thanks the Research Fellowship from the Japan Society for the Promotion of Science (JSPS) for Young Scientists. T.I. is a CEO of BNA Inc., the company that produces 2',4'-BNA^{NC} monomers. The other authors declared no conflict of interest.

1. Jones, P, Kafonek, S, Laurora, I and Hunninghake, D (1998). Comparative dose efficacy study of atorvastatin versus simvastatin, pravastatin, lovastatin, and fluvastatin in patients with hypercholesterolemia (the CURVES study). *Am J Cardiol* 81: 582–587.

2. Goldstein, JL and Brown, MS (2009). The LDL receptor. *Arterioscler Thromb Vasc Biol* **29**: 431–438.
3. Horton, JD, Goldstein, JL and Brown, MS (2002). SREBPs: activators of the complete program of cholesterol and fatty acid synthesis in the liver. *J Clin Invest* **109**: 1125–1131.
4. Horton, JD, Shah, NA, Warrington, JA, Anderson, NN, Park, SW, Brown, MS *et al.* (2003). Combined analysis of oligonucleotide microarray data from transgenic and knockout mice identifies direct SREBP target genes. *Proc Natl Acad Sci USA* **100**: 12027–12032.
5. Kong, WJ, Liu, J and Jiang, JD (2006). Human low-density lipoprotein receptor gene and its regulation. *J Mol Med* **84**: 29–36.
6. Issandou, M (2006). Pharmacological regulation of low density lipoprotein receptor expression: current status and future developments. *Pharmacol Ther* **111**: 424–433.
7. Zelcer, N and Tontonoz, P (2006). Liver X receptors as integrators of metabolic and inflammatory signaling. *J Clin Invest* **116**: 607–614.
8. Garcia, CK, Wilund, K, Arca, M, Zuliani, G, Fellin, R, Maioli, M *et al.* (2001). Autosomal recessive hypercholesterolemia caused by mutations in a putative LDL receptor adaptor protein. *Science* **292**: 1394–1398.
9. Harada-Shiba, M, Takagi, A, Miyamoto, Y, Tsushima, M, Ikeda, Y, Yokoyama, S *et al.* (2003). Clinical features and genetic analysis of autosomal recessive hypercholesterolemia. *J Clin Endocrinol Metab* **88**: 2541–2547.
10. Abifadel, M, Varret, M, Rabès, JP, Allard, D, Ouguerram, K, Devillers, M *et al.* (2003). Mutations in PCSK9 cause autosomal dominant hypercholesterolemia. *Nat Genet* **34**: 154–156.
11. Zelcer, N, Hong, C, Boyadjian, R and Tontonoz, P (2009). LXR regulates cholesterol uptake through Idol-dependent ubiquitination of the LDL receptor. *Science* **325**: 100–104.
12. Lambert, G, Charlton, F, Rye, KA and Piper, DE (2009). Molecular basis of PCSK9 function. *Atherosclerosis* **203**: 1–7.
13. Maxwell, KN, Soccio, RE, Duncan, EM, Sehayek, E and Breslow, JL (2003). Novel putative SREBP and LXR target genes identified by microarray analysis in liver of cholesterol-fed mice. *J Lipid Res* **44**: 2109–2119.
14. Attie, AD and Seidah, NG (2005). Dual regulation of the LDL receptor—some clarity and new questions. *Cell Metab* **1**: 290–292.
15. Cameron, J, Ranheim, T, Kulseth, MA, Leren, TP and Berge, KE (2008). Berberine decreases PCSK9 expression in HepG2 cells. *Atherosclerosis* **201**: 266–273.
16. Kong, W, Wei, J, Abidi, P, Lin, M, Inaba, S, Li, C *et al.* (2004). Berberine is a novel cholesterol-lowering drug working through a unique mechanism distinct from statins. *Nat Med* **10**: 1344–1351.
17. Kong, WJ, Wei, J, Zuo, ZY, Wang, YM, Song, DQ, You, XF *et al.* (2008). Combination of simvastatin with berberine improves the lipid-lowering efficacy. *Metab Clin Exp* **57**: 1029–1037.
18. Chan, JC, Piper, DE, Cao, Q, Liu, D, King, C, Wang, W *et al.* (2009). A proprotein convertase subtilisin/kexin type 9 neutralizing antibody reduces serum cholesterol in mice and nonhuman primates. *Proc Natl Acad Sci USA* **106**: 9820–9825.
19. Frank-Kamenetsky, M, Grefhorst, A, Anderson, NN, Racie, TS, Bramlage, B, Akinc, A *et al.* (2008). Therapeutic RNAi targeting PCSK9 acutely lowers plasma cholesterol in rodents and LDL cholesterol in nonhuman primates. *Proc Natl Acad Sci USA* **105**: 11915–11920.
20. Gupta, N, Fisker, N, Asselin, MC, Lindholm, M, Rosenbohm, C, Ørum, H *et al.* (2010). A locked nucleic acid antisense oligonucleotide (LNA) silences PCSK9 and enhances LDLR expression *in vitro* and *in vivo*. *PLoS ONE* **5**: e10682.
21. Swayze, EE, Siwkowski, AM, Wancewicz, EV, Migawa, MT, Wyrzykiewicz, TK, Hung, G *et al.* (2007). Antisense oligonucleotides containing locked nucleic acid improve potency but cause significant hepatotoxicity in animals. *Nucleic Acids Res* **35**: 687–700.
22. Yamamoto, T, Nakatani, M, Narukawa, K and Obika, S (2011). Antisense drug discovery and development. *Future Med Chem* **3**: 339–365.
23. Rahman, SM, Seki, S, Obika, S, Yoshikawa, H, Miyashita, K and Imanishi, T (2008). Design, synthesis, and properties of 2',4'-BNA(NC): a bridged nucleic acid analogue. *J Am Chem Soc* **130**: 4886–4896.
24. Obika, S, Rahman, SMA, Fujisaka, A, Kawada, Y, Baba, T and Imanishi, T (2010). Bridged nucleic acids: development, synthesis, and properties. *Heterocycles* **81**: 1347–1392.
25. Miyashita, K, Rahman, SMA, Seki, S, Obika, S and Imanishi, T (2007). N-Methyl substituted 2',4'-BNA(NC): a highly nuclease-resistant nucleic acid analogue with high-affinity RNA selective hybridization. *Chem Commun*: 3765–3767.
26. Prakash, TP, Siwkowski, A, Allerson, CR, Migawa, MT, Lee, S, Gaus, HJ *et al.* (2010). Antisense oligonucleotides containing conformationally constrained 2',4'-(N-methoxy) aminomethylene and 2',4'-aminooxymethylene and 2'-O,4'-C-aminomethylene bridged nucleoside analogues show improved potency in animal models. *J Med Chem* **53**: 1636–1650.
27. Graham, MJ, Lemonidis, KM, Whipple, CP, Subramaniam, A, Monia, BP, Crooke, ST *et al.* (2007). Antisense inhibition of proprotein convertase subtilisin/kexin type 9 reduces serum LDL in hyperlipidemic mice. *J Lipid Res* **48**: 763–767.
28. Yu, RZ, Baker, B, Chappell, A, Geary, RS, Cheung, E and Levin, AA (2002). Development of an ultrasensitive noncompetitive hybridization-ligation enzyme-linked immunosorbent assay for the determination of phosphorothioate oligodeoxynucleotide in plasma. *Anal Biochem* **304**: 19–25.
29. Straarup, EM, Fisker, N, Hedjäm, M, Lindholm, MW, Rosenbohm, C, Aarup, V *et al.* (2010). Short locked nucleic acid antisense oligonucleotides potently reduce apolipoprotein B mRNA and serum cholesterol in mice and non-human primates. *Nucleic Acids Res* **38**: 7100–7111.
30. Agrawal, S, Tamsamani, J and Tang, JY (1991). Pharmacokinetics, biodistribution, and stability of oligodeoxynucleotide phosphorothioates in mice. *Proc Natl Acad Sci USA* **88**: 7595–7599.
31. Phillips, JA, Craig, SJ, Bayley, D, Christian, RA, Geary, R and Nicklin, PL (1997). Pharmacokinetics, metabolism, and elimination of a 20-mer phosphorothioate oligodeoxynucleotide (CGP 69846A) after intravenous and subcutaneous administration. *Biochem Pharmacol* **54**: 657–668.
32. Lendvai, G, Velikyan, I, Bergström, M, Estrada, S, Laryea, D, Vällilä, M *et al.* (2005). Biodistribution of 68Ga-labelled phosphodiester, phosphorothioate, and 2'-O-methyl phosphodiester oligonucleotides in normal rats. *Eur J Pharm Sci* **26**: 26–38.
33. Akdim, F, Visser, ME, Tribble, DL, Baker, BF, Stroes, ES, Yu, R *et al.* (2010). Effect of mipomersen, an apolipoprotein B synthesis inhibitor, on low-density lipoprotein cholesterol in patients with familial hypercholesterolemia. *Am J Cardiol* **105**: 1413–1419.
34. Akdim, F, Stroes, ES, Sijbrands, EJ, Tribble, DL, Trip, MD, Jukema, JW *et al.* (2010). Efficacy and safety of mipomersen, an antisense inhibitor of apolipoprotein B, in hypercholesterolemic subjects receiving stable statin therapy. *J Am Coll Cardiol* **55**: 1611–1618.
35. Heemskerk, H, de Winter, C, van Kuik, P, Heuvelmans, N, Sabatelli, P, Rimessi, P *et al.* (2010). Preclinical PK and PD studies on 2'-O-methyl-phosphorothioate RNA antisense oligonucleotides in the mdx mouse model. *Mol Ther* **18**: 1210–1217.
36. Rudling, M (1992). Hepatic mRNA levels for the LDL receptor and HMG-CoA reductase show coordinate regulation *in vivo*. *J Lipid Res* **33**: 493–501.
37. Dueland, S, Drisko, J, Graf, L, Machleder, D, Lusic, AJ and Davis, RA (1993). Effect of dietary cholesterol and taurocholate on cholesterol 7 alpha-hydroxylase and hepatic LDL receptors in inbred mice. *J Lipid Res* **34**: 923–931.
38. Thomas, C, Pellicciari, R, Pruzanski, M, Auwerx, J and Schoonjans, K (2008). Targeting bile-acid signalling for metabolic diseases. *Nat Rev Drug Discov* **7**: 678–693.
39. Chiang, JY (2009). Bile acids: regulation of synthesis. *J Lipid Res* **50**: 1955–1966.
40. Pullinger, CR, Eng, C, Salen, G, Shefer, S, Batta, AK, Erickson, SK *et al.* (2002). Human cholesterol 7alpha-hydroxylase (CYP7A1) deficiency has a hypercholesterolemic phenotype. *J Clin Invest* **110**: 109–117.
41. Machleder, D, Ivandic, B, Welch, C, Castellani, L, Reue, K and Lusic, AJ (1997). Complex genetic control of HDL levels in mice in response to an atherogenic diet. Coordinate regulation of HDL levels and bile acid metabolism. *J Clin Invest* **99**: 1406–1419.
42. Miyake, JH, Duong-Polk, XT, Taylor, JM, Du, EZ, Castellani, LW, Lusic, AJ *et al.* (2002). Transgenic expression of cholesterol-7-alpha-hydroxylase prevents atherosclerosis in C57BL/6J mice. *Arterioscler Thromb Vasc Biol* **22**: 121–126.



Molecular Therapy–Nucleic Acids is an open-access journal published by Nature Publishing Group. This work is licensed under the Creative Commons Attribution-NonCommercial-No Derivative Works 3.0 Unported License. To view a copy of this license, visit <http://creativecommons.org/licenses/by-nc-nd/3.0/>

Supplementary Information accompanies this paper on the Molecular Therapy–Nucleic Acids website (<http://www.nature.com/mtna>)

Recent Progress in the Synthesis of Glycosyl Phosphate Derivatives

糖 -1- リン酸誘導体の合成化学の最近の進展

Oka, Natsuhisa¹; Sato, Kazuki²; and Wada, Takeshi²¹Department of Chemistry, Faculty of Engineering, Gifu University, 1-1 Yanagido, Gifu 501-1193, Japan²Department of Medical Genome Sciences, Graduate School of Frontier Sciences, The University of Tokyo,

5-1-5 Kashiwanoha, Kashiwa, Chiba 277-8562, Japan

FAX: 81-58-293-2564, E-mail: oka@gifu-u.ac.jp

(Received on May 31, 2012, accepted on July 9, 2012)

Key Words: glycosyl phosphate, phosphoglycan, H-phosphonate, boranophosphate, phosphoramidite**Abstract**

Phosphoglycans consisting of glycosyl phosphate repeating units have received much attention as synthetic targets mainly for their potential use as vaccines against pathogenic bacteria and protozoa. This review describes recent progress in the synthesis of glycosyl phosphates, especially of phosphoglycans, focusing on methods of synthesizing intersaccharide phosphodiester linkages.

要 約

糖 -1- リン酸繰り返し構造からなるホスホグリカンは、病原性細菌や寄生性原虫に対するワクチンなどとしての需要から、化学合成のターゲットとして注目を集めている。本総説では、このホスホグリカンを中心とする糖 -1- リン酸誘導体の化学合成に関する最近の研究について、リン酸ジエステル結合の合成法に焦点をあてて述べる。

A. Introduction

Phosphoglycans consisting of glycosyl phosphate repeating units are found in capsular polysaccharides (CPSs) and cell-wall lipopolysaccharides (LPSs) of bacteria, cell-wall and extracellular polysaccharides of yeasts, and surface glycocalyx and secreted glycoproteins of protozoan parasites (1). Because these polysaccharides and glycoconjugates define the immunological specificity of the parent microorganism, the primary constituent phosphoglycans have been studied as potential vaccines, particularly against virulent species such as *Neisseria meningitidis*, *Streptococcus pneumoniae*, and *Leishmania* (Fig. 1) (2–5). In fact, the CPSs isolated from *N. meningitidis* and *S. pneumoniae* as well as their conjugates with proteins are used as vaccines (2, 3). Furthermore, the CPSs of bacteria as well as the glycocalyx and secreted glycoproteins of parasites play important roles in infection and the evasion of the host innate defense, contributing to the virulence of these microorganisms. For this reason, the structure–activity relationship and biosynthesis of these polysaccharides and glycoconjugates have also been important subjects of research (1, 6–8). In addition, glycosyl phosphates are the primary constituents of glycosyl donors in the biosynthesis of carbohydrates, such as sugar nucleotides (9, 10) and dolichol phosphate sugars (11, 12). Sugar nucleotides are useful for the enzymatic synthesis of oligosaccharides and glycosides (13, 14). Chemically modified analogs of these

A. はじめに

糖 -1- リン酸繰り返し構造からなるホスホグリカン、細菌の莢膜多糖や細胞壁リポ多糖、酵母の細胞壁多糖や細胞外多糖、寄生性原虫の糖衣や分泌糖タンパク質などに含まれる(1)。これらの多糖や複合糖質は、多くの場合抗原決定基として働くことから、その中心構造であるホスホグリカンは、特に感染被害の大きい髄膜炎菌、肺炎球菌、リーシュマニアなどに由来するもの(図1)を対象に、ワクチンとしての応用を指向した研究が行われてきた(2–5)。実際に、髄膜炎菌や肺炎球菌から抽出精製した莢膜多糖やそのタンパク質との複合体はワクチンとして用いられている(2,3)。また、細菌の莢膜多糖や寄生虫の糖衣、及び分泌糖タンパク質は、これらの病原体の宿主への感染や宿主内での免疫機構の回避などにおいて重要な役割を担い、病原性の一因となっている。そのため、これらの主構成要素であるホスホグリカンの分子構造と機能の関係や、生合成経路に関しても重要な研究対象となっている(1,6–8)。加えて、糖 -1- リン酸は、糖ヌクレオチド(9,10)やドリコールリン酸糖(11,12)など、生体内で働く糖供与体の基本構造でもある。糖ヌクレオチドは、酵素を用いた糖鎖や配糖体などの合成原料として用いられる(13,14)。また、これらの生体内糖供与体の化学修飾アナログは、糖鎖の生合成経路をターゲットとするプローブや阻害剤としても有用である